R. & M. No. 3785

R. & M. No. 3785

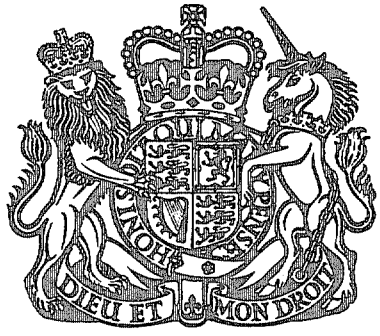

PROCUREMENT EXECUTIVE, MINISTRY OF DEFENCE
AERONAUTICAL RESEARCH COUNCIL
REPORTS AND MEMORANDA

Some Series-Expansion Solutions for Slender Wings with Leading-Edge Separation

By R. W. CLARK, J. H. B. SMITH and C. W. THOMPSON
Aerodynamics Dept., R.A.E., Farnborough

ESTABLISHMENT
BEDFORD.

LONDON: HER MAJESTY'S STATIONERY OFFICE
1976
£4·30 net

Some Series-Expansion Solutions for Slender Wings with Leading-Edge Separation

By R. W. CLARK, J. H. B. SMITH and C. W. THOMPSON*

Aerodynamics Dept., R.A.E., Farnborough

Reports and Memoranda No. 3785†
January, 1975

Summary

The vortex formed above each leading edge of the wing is represented by a line vortex, as in the treatment of the flat delta wing by Brown and Michael, and the slender-body approximation is made. Four problems are treated: the thick, conical delta wing with rhombic cross-sections; the thick, conically-cambered delta wing formed by one-half of a circular cone; the flat-plate wing with curved leading edges; and a wing with a partially unswept leading edge and lengthwise camber. The quantities of interest are the position of the vortex and its circulation, and the non-linear lift and pitching moment of the wing. In each problem the solution is presented as an asymptotic series in a small parameter representing the scale of the separation. The solutions are used to shed light on a number of problems arising in the aerodynamics of slender wings.

* University of Cambridge. This work was begun while C.W.T. was a vacation student at R.A.E. in Summer, 1973.

† Replaces R.A.E. Technical Report 75004-A.R.C. 36 059

LIST OF CONTENTS

1. Introduction

It is generally accepted that an adequate model of the flow past a slender wing with leading-edge separation must include some representation of that part of the shear layer shed from the leading edge which lies close to the edge, as well as a representation of the part which is rolled up into a vortex. The present Report, on the other hand, treats the simple model, due to Brown and Michael[1], in which the entire shear layer is represented by a line-vortex in a potential flow, with a force-carrying cut connecting the line-vortex to the leading edge.

There are two reasons for this. The first is that two recent papers by Barsby[2,3] have indicated that, provided the scale of the separation is very small, it makes little difference to the overall behaviour of the flow whether a length of vortex sheet representing the shear layer near the leading edge is included or not. Earlier calculations with the vortex-sheet model[4] were not carried to small enough angles of incidence for this feature to be observed. Even now, the agreement between the line-vortex and the vortex-sheet models rests on numerical calculations rather than mathematical argument. However, the numerical evidence for the convergence of the results of the vortex-sheet calculations to the results of the line-vortex calculations, as the incidence (relative to the attached flow condition) tends to zero, is strong, both for the flat-plate delta[3] and for the thin delta with conical camber[2]; so it seems justifiable to make use of the line-vortex model for circumstances in which the separation is small. In particular, the leading terms in an expansion in terms of a parameter representing the scale of the separation may well be relevant to the real flow.

The other reason is the much greater simplicity of the line-vortex model. In particular, for small separations, it is possible to obtain asymptotic expansions for the solution of the equations governing the line-vortex model. This has not so far proved possible with the vortex-sheet model. Moreover, as the scale of the separation becomes smaller, extra difficulties arise in the numerical treatment of the vortex-sheet model, first the appearance of inflections in the sheet shape[4] and then the movement of the separation line inboard of the leading edge[3]. Thus the line-vortex model has the greatest advantage in simplicity over the vortex-sheet model for the small-scale separations for which it is also most accurate.

There is a further general point to be made about the model. Because the separation line lies inboard of the leading edge for small angles of incidence, the line-vortex model becomes inconsistent, since it involves representing part of the vortex sheet by a cut which joins the vortex to the leading edge, rather than to the actual separation line. Smith[5] has recently re-examined the original problem of the flat-plate delta wing, allowing the cut to join the vortex to the predicted inviscid separation line, and found the solution to be very little affected. In particular, the leading terms of the expansion of the solution in powers of the angle of incidence were unchanged. It seems therefore that the inconsistency can be disregarded and the model used in its original simple form. This is confirmed in the present Report for a wing with thickness (*see* Section 2.3).

The other limiting feature of the present approach, and of all the work that has been done with the vortex-sheet model, is the use of slender-body theory. This means that quantitative agreement with experimental measurements can only be expected in fairly special circumstances, regardless of whether the flow is separated or attached. At low speeds, the flow over the forward part of a slender wing is described successfully, but overall forces and moments cannot be reliably predicted, as the upstream influence of the trailing edge on the flow is not represented in the model. As the aspect ratio falls, particularly for planforms with streamwise tips, or the free-stream Mach number rises towards one, the upstream influence of the trailing edge becomes less significant, and the quantitative predictions of slender-body theory are approached. At free-stream Mach numbers in the neighbourhood of one, there is evidence that lift and pitching moment are predicted correctly. Quantitative predictions become unreliable again at moderate supersonic speeds, essentially because the theory allows disturbances to propagate across the whole cross-flow plane, instead of confining them to the downstream Mach cone or conoid. In spite of these deficiencies, slender-body theory can provide a useful indication of effects which can only be calculated in detail by very elaborate treatments; in particular, it makes the representation of leading-edge separation relatively straightforward.

In the present Report, the line-vortex model of leading-edge separation is applied, within the framework of slender-body theory, to four problems. In each case a solution is obtained in the form of asymptotic expansions for the position and circulation of the vortex and the lift and pitching moment of the configuration, for small values of a parameter representing the scale of the separation.

The first configuration is the thick delta wing in the form of a cone with rhombic cross-sections. This has already been treated by the vortex-sheet model[6], but the representation used did not allow solutions to be obtained at small angles of incidence. The expansions now obtained for small incidence supplement the previous work[6] and that of Ref. 7, in which a treatment valid for thin cones was presented. The loci of the centre of the vortex for the thicker wings treated in Ref. 6 show a curious feature at the lower end of the incidence range for which solutions could be obtained; after tending steadily towards the leading edge as the

incidence falls, the locus of the vortex centre appears to turn towards the wing surface, as shown in Fig. 3. The present treatment predicts a smooth and regular variation of the position of the line vortex in the neighbourhood of the leading edge, suggesting that the anomaly in the earlier calculations is due to an inadequacy of the numerical representation. A question that can be answered is that raised by Barsby[3], as to whether the inboard occurrence of separation is only predicted for wings of vanishing edge angle. The present treatment shows that inboard separation is to be expected for wings of finite thickness, provided the edge angle is not too great; for rhombic cones inboard separation is predicted for small angles of incidence provided the edge angle is less than 42·5 degrees.

The second configuration is also a thick, conical delta wing, but it incorporates conical camber, since it consists of one-half of a circular cone. This was treated in attached flow by Portnoy[8]. When the half-cone is placed with its flat lower surface at a positive angle of incidence to the stream, there is one angle of incidence at which the flow has no tendency to separate from the leading edge. This is referred to as the attachment incidence. At other angles of incidence the scale of the separation will be related to the difference between the actual incidence and the attachment incidence, and it is this difference which is used as the small parameter in the asymptotic expansion of the solution. The results obtained can be related to those found for the rhombic cone with the same edge angle ($\pi/2$), so verifying Maskell's similarity theory[9] in a particular case. The configuration is of interest because the apex regions of warped slender wings combine appreciable cross-sectional thickness and camber in a similar way. Ref. 10 shows that a half-cone produces more lift at its attachment incidence than would be expected if it were regarded as a combination of a warped mean surface and a symmetrical distribution of volume. The present results show that the leading-edge separation from the half-cone produces less extra lift for the same increment in incidence above the attachment condition than does the rhombic cone with the same edge angle, at least when this increment is small. The lift increment due to the separation is the same in magnitude whether the increment in incidence is positive or negative.

The third configuration is the flat-plate slender wing with curved leading edges and a straight, unswept, trailing edge. This has previously been treated by Smith[11], using the line-vortex model of the flow and a numerical method for the downstream integration of the ordinary differential equations to which the model gives rise in this case. Clark is currently improving on this work by applying the vortex-sheet model of the flow to wings with curved leading edges and lengthwise camber. In the present Report the differential equations governing the line-vortex model for the plane wing are expanded for small values of the angle of incidence, leading to much simpler differential equations for the coefficients of the leading terms. These simpler equations are integrated in closed form. Difficulties arise when the leading edges become streamwise and these are overcome by the use of matched asymptotic expansions. The solutions found confirm that separation can have a large effect on lift-curve slope and aerodynamic centre at small angles of incidence. The form of the solution also suggests an improvement in the usual method for obtaining the lift slope and aerodynamic centre at zero lift from wind-tunnel measurements on slender wings.

The fourth configuration studied is only expected to be of interest in relation to a more complex situation. Consider a slender wing with longitudinal camber, but plane cross-sections, placed at an overall angle of incidence such that its local inclination to the free stream passes through zero somewhere along its length. Then the vortices formed near the apex cease to be fed from the leading edges at some station near that of zero local inclination. At about the same station vortices of the opposite sense begin to form on the opposite surface of the wing. Jones[12] shows a water-tunnel visualization of the flow past a delta wing with positive camber at zero overall incidence (i.e. the apex and trailing edge in the same horizontal plane, with the rest of the wing above them). Air is injected into the vortices, which become visible as hollow cores below the lower surface over the forward half of the wing and above the upper surface over the rearward half. No continuation of the apex vortices on the lower surface over the rear half is visible, probably because the pressure in them rises, so that the air finds its way, under the influence of pressure gradients rather than shear stresses, into the new vortices on the upper surface instead. This gives the impression that the vortices are being convected round the edge. Nangia and Hancock[13] also interpret their oil-flow visualizations in this way. The present authors believe, on the evidence of recent smoke and tuft explorations in the No. 1 $11\frac{1}{2}$ ft $\times 8\frac{1}{2}$ ft tunnel, that this impression is misleading; and that, towards the rear of the wing, there are four vortices, one above and one below each panel of the wing, with opposite senses of rotation. This view is supported by Snyder[14], who observed the vortex cores through the condensation of steam injected into them.

Recent, as yet unpublished, calculations by Clark, using the vortex-sheet model, provide some insight into the early stages of the phenomenon, upstream of the station at which the local inclination is zero. To proceed further downstream a representation of the second vortex must be introduced. This originates at a lengthwise station at which the span is finite, and at which an effective local incidence vanishes. Its initial growth is therefore likely to be the same as that of a vortex formed from the swept part of the leading edge of a truncated

slender wing (*see* Fig. 11), which has straight cross-sections and a form of lengthwise camber leading to zero local incidence along the unswept part of the leading edge. This is the fourth configuration studied. Solutions are obtained as asymptotic expansions in the distance downstream from the unswept part of the leading edge, which governs the scale of the separation. Different forms arise depending on the relative rates of growth of the local span and the local incidence in the downstream direction. Similar problems involving the formation of vortices from stations at which the span is finite but the incidence is zero are likely to arise on slender wings undergoing pitching motions which take them through zero incidence.

The remaining sections of the Report deal with each of these four configurations. Each section can be read independently, though the principal symbols, the references and the figures are grouped at the end of the Report in the usual way.

2. The Rhombic Cone

In the Brown and Michael[1] model of flow over wings with leading-edge separation, the rolled-up vortex sheet which forms over each leading edge of the wing is modelled by a line-vortex. According to slender-body theory the solution can be derived by considering the flow in the cross-sectional plane perpendicular to the axis of the wing, with suitable boundary conditions representing the flow at infinity and representing the growth of the wing cross-section in the streamwise direction. In this cross-flow plane the line-vortex becomes an isolated point-vortex, and a cut is introduced joining this point to the leading edge in order to ensure that the velocity potential defining the flow is single-valued. The solution can then be determined by finding the position and strength of this vortex which satisfies the conditions that the velocity is finite at the leading edge and that the total force acting on the vortex and the cut is zero.

This section deals with the flow over thick conical wings with rhombic cross-sections. These wings were examined by Smith[6] using the more detailed vortex-sheet model, so the conformal transformation used to derive the complex velocity potential follows immediately from this work.

Fig. 1 shows the configuration with the origin of the coordinates at the wing apex and the x-axis along the wing centre line. It also serves to define the angles δ and $\varepsilon\pi$.

2.1. Formal Solution

The wing cross-section and the right-hand vortex are shown in Fig. 2a. The conformal transformation

$$Z = s + \int_0^{\omega} \left(\frac{t^2}{t^2+d^2}\right)^{\varepsilon} dt \tag{1}$$

maps the wing into the slit AC on the imaginary axis in the ω-plane as shown in Fig. 2b. From equation (1) we can show that the lengths s and d are related in terms of the beta function by

$$\frac{s}{d} = \tfrac{1}{2} \sin \varepsilon\pi \, B(\varepsilon + \tfrac{1}{2}, 1-\varepsilon) \quad . \tag{2}$$

The complex conjugate velocity also follows immediately from Ref. 6 by omitting the contribution arising from the vortex sheet, so that, if W is the complex velocity potential

$$\frac{dW}{d\omega} = -i\alpha U + \frac{KU \cos \varepsilon\pi}{i\pi} \int_{-id}^{id} \left|\frac{t^2}{t^2+d^2}\right|^{\varepsilon} \frac{dt}{\omega - t} + \frac{\Gamma}{2\pi i}\left(\frac{1}{\omega - \omega_v} - \frac{1}{\omega + \bar{\omega}_v}\right) \quad . \tag{3}$$

In this expression α denotes the angle between the wing axis and the free stream, so that the first term represents the required behaviour at infinity. The second term is the attached-flow solution satisfying the wing boundary condition, whilst the third term is due to the vortex of strength Γ at ω_v and its image in the imaginary axis.

We introduce the following non-dimensional quantities

$$\omega_1 = \omega_v / d \quad ,$$
$$a = \alpha / K$$

and

$$\gamma = \Gamma/(KUd) \quad . \tag{4}$$

Since $d\omega/dZ$ is infinite at the leading edge, by equation (1), the condition that the velocity there should be finite requires that $dW/d\omega = 0$ at $\omega = 0$, which leads to

$$\gamma = 2\pi a \frac{\omega_1 \bar{\omega}_1}{\omega_1 + \bar{\omega}_1} \quad . \tag{5}$$

The expression for the force on the vortex and cut is derived by Smith[4] for the vortex-sheet model, and the only difference in this case is that the cut ends at the leading edge of the wing. The zero-force condition is therefore

$$\lim_{Z \to Z_v} \left(\frac{dW}{dZ} - \frac{\Gamma}{2\pi i} \frac{1}{Z - Z_v} \right) = \frac{KU}{s} (2\bar{Z}_v - s) \quad , \tag{6}$$

where Z_v is the position of the right-hand vortex in the Z-plane.

Substituting from equations (1) and (3) into this last condition gives, after some manipulation,

$$-ia + \frac{\cos \varepsilon\pi}{i\pi} \int_{-i}^{i} \left| \frac{t^2}{t^2+1} \right|^{\varepsilon} \frac{dt}{\omega_1 - t} - \frac{\gamma}{2\pi i} \left(\frac{\varepsilon}{\omega_1 (1+\omega_1^2)} + \frac{1}{\omega_1 + \bar{\omega}_1} \right) = \left(\frac{\omega_1^2}{1+\omega_1^2} \right)^{\varepsilon} \left(2\frac{\bar{Z}_v}{s} - 1 \right) \quad . \tag{7}$$

Eliminating the circulation from equation (7), using equation (5), leads to

$$\frac{ia}{(\omega_1 + \bar{\omega}_1)^2} \left(\omega_1^2 + \bar{\omega}_1 (\omega_1 + \bar{\omega}_1) \left(1 - \frac{\varepsilon}{1+\omega_1^2} \right) \right)$$
$$= \frac{\cos \varepsilon\pi}{i\pi} \int_{-i}^{i} \left| \frac{t^2}{t^2+1} \right|^{\varepsilon} \frac{dt}{\omega_1 - t} - \left(\frac{\omega_1^2}{1+\omega_1^2} \right)^{\varepsilon} \left(2\frac{\bar{Z}_v}{s} - 1 \right) \quad , \tag{8}$$

which along with equation (1) is sufficient to determine the vortex position.

2.2 Asymptotic Expansion for Small Incidence

Rather than obtaining solutions to equations (5) and (8) this present report examines these equations for small values of the incidence parameter a, and obtains expansions in ascending powers of a for the vortex strength and position. Initially, we make the assumption that, as the angle of incidence decreases to zero, the vortex position tends to the leading edge, so that $\omega_1 \to 0$ as $a \to 0$.

Using Appendix C of Ref. 6 the attached-flow contribution in equation (8) can be expanded for small ω_1 to give

$$\frac{\cos \varepsilon\pi}{i\pi} \int_{-i}^{i} \left| \frac{t^2}{t^2+1} \right|^{\varepsilon} \frac{dt}{\omega_1 - t} = \left(\frac{\omega_1^2}{1+\omega_1^2} \right)^{\varepsilon} (1 - B_0 \omega_1^{1-2\varepsilon} + B_1 \omega_1^{3-2\varepsilon} + \ldots) \quad , \tag{9}$$

where

$$B_0 = \frac{\cos \varepsilon\pi}{\pi(1-2\varepsilon)} B(\tfrac{1}{2}+\varepsilon, 1-\varepsilon) \quad \text{and} \quad B_1 = \frac{1-\varepsilon}{3-2\varepsilon} \frac{\cos \varepsilon\pi}{\pi} B(\tfrac{1}{2}+\varepsilon, 1-\varepsilon) \quad .$$

Also, from equation (1),

$$\frac{Z_v}{s} = 1 + \frac{d}{s} \omega_1^{1+2\varepsilon} \left(\frac{1}{1+2\varepsilon} - \frac{\varepsilon}{3+2\varepsilon} \omega_1^2 + \ldots \right) \quad . \tag{10}$$

Substituting equations (9) and (10) into (8) yields

$$\frac{ia}{(\omega_1 + \bar{\omega}_1)^2} \left(\omega_1^2 + \bar{\omega}_1 (\omega_1 + \bar{\omega}_1) \left(1 - \frac{\varepsilon}{1+\omega_1^2} \right) \right) = -B_0 \omega_1 - \frac{2d}{(1+2\varepsilon)s} |\omega_1|^{4\varepsilon} \bar{\omega}_1 + (B_1 + \varepsilon B_0) \omega_1^3 + \ldots \quad . \tag{11}$$

Introducing the real and imaginary components of $\omega_1 = \sigma + i\tau$ enables equation (11) to be written as

$$\frac{ia}{4\sigma^2}(3\sigma^2-\tau^2-2\varepsilon\sigma(\sigma-i\tau)+2\varepsilon\sigma(\sigma^2+\tau^2)(\sigma+i\tau)+\ldots)$$

$$= -B_0(\sigma+i\tau)-\frac{2d}{(1+2\varepsilon)s}(\sigma^2+\tau^2)^{2\varepsilon}(\sigma-i\tau)+(B_1+\varepsilon B_0)(\sigma^3-3\sigma\tau^2+i\tau(3\sigma^2-\tau^2))+\ldots \quad . \tag{12}$$

If we look initially at the leading terms on each side of this equation we find that

$$\sigma=\frac{\varepsilon k}{2B_0}a \quad \text{and} \quad \tau=\frac{\varepsilon k^2}{2B_0}a \tag{13}$$

where $k=\sqrt{(3-2\varepsilon)/(1-2\varepsilon)}$. The thickness parameter ε must satisfy $0<\varepsilon<\frac{1}{2}$ with the value $\varepsilon=\frac{1}{2}$ corresponding to the thin wing. It can be seen that, for $\varepsilon=\frac{1}{2}$, k becomes infinite and the above expansion will break down. The thin-wing expansion is therefore not a uniform limit of this expansion, and this point is taken up again in Subsection 2.4. The reason for this non-uniformity appears to be that the boundary condition which must be satisfied on the surface of the thick wing determines the lateral velocity at the leading edge, whereas this is not determined for the thin wing. The behaviour of the real flow will be affected by the way in which the boundary layers on the upper and lower surfaces blend into the free shear layer.

Examination of the terms involved in equation (11) suggests that we seek an expansion of the form

$$\omega_1 = a\sum_{i,j=0}^{\infty} p_{ij}a^{2i+4j\varepsilon} \tag{14}$$

where the p_{ij} will be complex constants. The first of these constants follows immediately from equation (13), and if we substitute the expansion (14) into equation (12) the next two terms in the series can be derived. Thus

$$p_{00}=\frac{\varepsilon k}{2B_0}(1+ik) \quad , \tag{15a}$$

$$p_{01}=-\frac{\varepsilon kd}{B_0^2(1-4\varepsilon^2)s}\left(\frac{\varepsilon^2k^2}{4B_0^2}(1+k^2)\right)^{2\varepsilon}(1+ik(1+2\varepsilon)) \tag{15b}$$

and

$$p_{10}=\frac{\varepsilon^3 k}{2B_0^3(1-2\varepsilon)^2}(1-2\varepsilon+ik(1-2\varepsilon^2)) \quad . \tag{15c}$$

Substitution of the expansion (14) into equations (10) and (5) enables us to find the vortex position and strength in terms of these coefficients. This gives

$$Z_v = s+dp_{00}^{2\varepsilon}a^{1+2\varepsilon}\left(\frac{p_{00}}{1+2\varepsilon}+p_{01}a^{4\varepsilon}+\left(p_{10}-\frac{\varepsilon p_{00}^3}{3+2\varepsilon}\right)a^2+\ldots\right) \tag{16}$$

and

$$\gamma=\frac{2\pi a^2}{p_{00}+\bar{p}_{00}}\left(|p_{00}|^2+\frac{p_{01}\bar{p}_{00}^2+\bar{p}_{01}p_{00}^2}{p_{00}+\bar{p}_{00}}a^{4\varepsilon}+\frac{p_{10}\bar{p}_{00}^2+\bar{p}_{10}p_{00}^2}{p_{00}+\bar{p}_{00}}a^2+\ldots\right) \quad . \tag{17}$$

An expression for the lift on this wing was derived in Appendix B of Ref. 6, and from it the lift coefficient is given as

$$\frac{C_L}{\alpha K}=4\left(\frac{\pi\varepsilon d^2}{s^2}-\cot\varepsilon\pi\right)+\frac{4d^2}{s^2}\frac{\gamma\sigma}{a} \quad . \tag{18}$$

Incorporating the expansions given by equations (15) and (17) we find that

$$\frac{C_L}{\alpha K}=4\left(\frac{\pi\varepsilon d^2}{s^2}-\cot\varepsilon\pi\right)+a^2\frac{4\pi d^2\varepsilon^2(3-2\varepsilon)(1-\varepsilon)}{B_0^2 s^2(1-2\varepsilon)^2}\times$$
$$\times\left(1-\frac{2d(2+\varepsilon-2\varepsilon^2)}{B_0 s(1-4\varepsilon^2)(1-\varepsilon)}\left(\frac{\varepsilon^2k^2(1+k^2)}{4B_0^2}\right)^{2\varepsilon}a^{2\varepsilon}+\frac{\varepsilon^2(2-\varepsilon-2\varepsilon^2)}{B_0^2(1-2\varepsilon)^2}a^2\right) \quad . \tag{19}$$

It is clear that the coefficient of a^2 in this expression becomes very large as $\varepsilon\to\frac{1}{2}$, that is as the wing becomes very thin. This implies that the range of values of a for which this approximation is useful becomes very small for thinner wings. The meaning of 'thinner' in this context can only be made clear by quoting numerical values. For $\varepsilon=0{\cdot}25$, corresponding to an edge angle of 90 degrees, the coefficient of a^2 in equation (19) is about 6 times the constant term, while for $\varepsilon=0{\cdot}45$, corresponding to an edge angle of 18 degrees, this ratio has increased to 56. The inclusion of the higher order terms, $a^{2+2\varepsilon}$ and a^4, can only partially alleviate this since the coefficients of these terms become very large as $\varepsilon\to\frac{1}{2}$. It seems therefore that this expansion is of little use for the calculation of non-linear lift at angles of incidence which are of practical interest. An expansion of wider validity is obtained in Subsection 2.4.

In the derivation of these expansions it was assumed that as the angle of incidence vanished the vortex would tend towards the leading edge. However, in the numerical work by Smith[6] on the vortex-sheet model, it was found that, for smaller values of ε, as the incidence decreased the vortex appeared at first to be approaching the leading edge, but then for smaller angles of incidence it began to turn inboard and away from the leading edge. This is shown in Fig. 3 for the case in which $\varepsilon=1/6$. It was therefore thought worthwhile to look for an alternative expansion in which the vortex tends to some other point on the wing surface. This was done by assuming an expansion for the vortex position about a general point on the wing surface and by assuming an expansion about the wing centre line. Details of these calculations are given in Appendix A. However, both these assumptions led to contradictions and so the conclusion is that the only valid expansion for small incidence is that given by equations (16) and (17), and the deviation found in the earlier numerical results cannot be explained in terms of this simplified model.

2.3 Inboard Separation

It was found by Barsby[3] in his application of the vortex-sheet model to the flow over thin wings that, at low incidences, the separation did not occur at the leading edge but at a point inboard of, although still close to, the leading edge. This striking result invites speculation as to whether a similar behaviour might be observable in a real flow. It was suggested in Ref. 3 that this phenomenon might be peculiar to wings of vanishing thickness, and so it was thought to be worthwhile to examine the present solution for the thick wing to see whether such inboard separation could occur.

First of all it is necessary to check whether the solution given in the preceding section is consistent with separation from the leading edge, that is, whether the flow on the upper surface just inboard of the leading edge is directed outwards across the conical rays. Therefore using equation (3), we derive an expansion for the velocity valid for $|\omega|\ll|\omega_v|$. Thus

$$\frac{1}{\omega-\omega_v}-\frac{1}{\omega+\bar{\omega}_v}=-\left(\frac{1}{\omega_v}+\frac{1}{\bar{\omega}_v}\right)\left(1+\left(\frac{1}{\omega_v}-\frac{1}{\bar{\omega}_v}\right)\omega+\ldots\right)$$
$$=-\frac{2\pi a}{\gamma d}\left(1-\frac{2\pi i}{\sigma^2+\tau^2}\frac{\omega}{d}+\ldots\right) \quad , \tag{20}$$

where we have made use of equation (5). Retaining the first two terms in equation (9) and noting that

$$\frac{d\omega}{dZ}=\left(\frac{d^2+\omega^2}{\omega^2}\right)^{\varepsilon} \quad , \tag{21}$$

we are led to the following expression for the conjugate velocity

$$\frac{1}{KU}\frac{dW}{dZ}=1+\left(\frac{2a\tau}{\sigma^2+\tau^2}-B_0\right)\left(\frac{\omega}{d}\right)^{1-2\varepsilon}+\ldots \quad . \tag{22}$$

Substituting the leading terms for σ and τ given in (13) gives

$$\frac{1}{KU}\frac{dW}{dZ}=1+B_0\frac{1-3\varepsilon+\varepsilon^2}{\varepsilon(1-\varepsilon)}\left(\frac{\omega}{d}\right)^{1-2\varepsilon}+\ldots \quad . \tag{23}$$

Since a point on the upper surface of the wing corresponds to ω lying on the upper half of the imaginary axis the velocity on the wing is

$$\frac{1}{KU}\frac{dW}{dZ}=1+B_0\frac{1-3\varepsilon+\varepsilon^2}{\varepsilon(1-\varepsilon)}\left|\frac{\omega}{d}\right|^{1-2\varepsilon}(\sin\varepsilon\pi+i\cos\varepsilon\pi) \quad . \tag{24}$$

The flow will cross the conical ray in the outward direction if the horizontal component of the velocity is greater than

$$KUy/s=KU(1-(s-y)/s) \quad ,$$

and, since $B_0>0$, comparison of this expression with (24) shows that this condition will certainly be satisfied if

$$1-3\varepsilon+\varepsilon^2>0 \quad . \tag{25}$$

If, on the other hand, $1-3\varepsilon+\varepsilon^2<0$ then the condition required for outboard separation will be that, close to the leading edge,

$$\frac{B_0|1-3\varepsilon+\varepsilon^2|}{\varepsilon(1-\varepsilon)}\sin\varepsilon\pi\left|\frac{\omega}{d}\right|^{1-2\varepsilon}<\frac{s-y}{s} \quad . \tag{26}$$

But on the wing surface close to the leading edge it follows from equation (10) that

$$\frac{s-y}{s}\sim\frac{d\sin\varepsilon\pi}{s(1+2\varepsilon)}\left|\frac{\omega}{d}\right|^{1+2\varepsilon} \quad ,$$

and for $|\omega|$ sufficiently small $|\omega|^{1+2\varepsilon}\ll|\omega|^{1-2\varepsilon}$ and so (26) cannot be satisfied close to the leading edge. The inequality (25) is therefore a necessary and sufficient condition for outboard separation to occur. Since we are interested only in values of ε less than 0·5, it follows that separation takes place from the leading edge if and only if

$$\varepsilon<\varepsilon_0=\tfrac{1}{2}(3-\sqrt{5}) \quad . \tag{27}$$

This means that for wings on which the leading-edge angle is less than $(1-2\varepsilon_0)\pi$ radians, or about 42·5 degrees, this model of the flow will predict an inboard separation as was found for the thin wing, but for wings thicker than this the flow separation will take place at the leading edge. The solution given in the preceding section is therefore only strictly consistent for thicker wings with the outboard separation. However Smith[5] found that the modification necessary to make the solution consistent in the case of the flat-plate wing did not affect the leading term in the asymptotic expansion, and we will verify that this is still true for the thick wings dealt with here.

If we denote the position of the separation line in the cross-flow plane by χ and assume that the cut joins the vortex to this point then, as in Ref. 5, the only term in equation (8) to be altered will be that due to the force on the cut. This equation can therefore be written

$$\frac{ia}{(\omega_1+\bar{\omega}_1)^2}\left(\omega_1^2+\bar{\omega}_1(\omega_1+\bar{\omega}_1)\left(1-\frac{\varepsilon}{1+\omega_1^2}\right)\right)=\frac{\cos\varepsilon\pi}{i\pi}\int_{-i}^{i}\left|\frac{t^2}{t^2+1}\right|^{\varepsilon}\frac{dt}{\omega_1-t}-\left(\frac{\omega_1^2}{1+\omega_1^2}\right)^{\varepsilon}\left(\frac{2\bar{Z}_v-\bar{\chi}}{s}\right) \quad . \tag{28}$$

The additional condition necessary to determine χ is that χ should lie on a separation line, and this can be written, as in Ref. 5, as

$$\frac{1}{KU}\frac{dW}{dZ}\bigg|_{Z=\chi}=\frac{\bar{\chi}}{s} \quad . \tag{29}$$

Suppose that the separation point in the ω-plane is given by $i\mu d$. Then from equation (1)

$$\frac{s-\bar{\chi}}{s}=(\sin\varepsilon\pi+i\cos\varepsilon\pi)\frac{d}{s}\int_0^{\mu}\left(\frac{t^2}{1-t^2}\right)^{\varepsilon}dt \quad , \tag{30}$$

and so comparison of equations (8) and (11) enables (28) to be written as

$$\frac{ia}{(\omega_1+\bar{\omega}_1)^2}\left(\omega_1^2+\bar{\omega}_1(\omega_1+\bar{\omega}_1)\left(1-\frac{\varepsilon}{1+\omega_1^2}\right)\right)$$
$$=-B_0\omega_1+\frac{d}{s}\frac{\sin\varepsilon\pi+i\cos\varepsilon\pi}{1+2\varepsilon}\mu^{1+2\varepsilon}\omega_1^{2\varepsilon}-\frac{2d}{s}\frac{|\omega_1|^{4\varepsilon}\bar{\omega}_1}{1+2\varepsilon}+(B_1+\varepsilon B_0)\omega_1^3+\ldots \quad . \tag{31}$$

A consistent solution to this equation and (29) for the vortex strength and position can be obtained if we make the physically realistic assumption that μ will be of the same order or smaller than $|\omega_1|$. The leading term in equation (31) will then be unaffected by the presence of the inboard separation and the leading term in the expansion for the vortex position will be given by (13).

The position of the separation line can now be determined from equation (29), which can be written, with the aid of equations (1), (3), (5) and (30) as

$$-\frac{ia(i\mu(\omega_1-\bar{\omega}_1)+\mu^2)}{(\omega_1-i\mu)(\bar{\omega}_1+i\mu)}+\frac{\cos\varepsilon\pi}{i\pi}\int_{-i}^{i}\left|\frac{t^2}{1+t^2}\right|^{\varepsilon}\frac{dt}{i\mu-t}$$
$$=\left(\frac{-\mu^2}{1-\mu^2}\right)^{\varepsilon}\left(1-\frac{d}{s}(\sin\varepsilon\pi+i\cos\varepsilon\pi)\int_0^{\mu}\left(\frac{t^2}{1-t^2}\right)^{\varepsilon}dt\right) \quad . \tag{32}$$

Introducing σ and τ for the real and imaginary parts of ω_1 and using equation (9) to find an expansion for the integral on the left-hand side gives

$$\frac{a(2\tau-\mu)}{\sigma^2+(\tau-\mu)^2}=B_0-\frac{d}{s}\frac{\mu^{4\varepsilon}}{1+2\varepsilon}+(B_1+\varepsilon B_0)\mu^2+\ldots \quad . \tag{33}$$

If we retain only the leading term in the right-hand side of this equation and use equation (13) for σ and τ, then we find that

$$\mu=\frac{a}{2B_0}(\varepsilon k^2-1\pm\sqrt{(1+\varepsilon(2-\varepsilon)k^2)}) \quad . \tag{34}$$

The positive sign gives rise to a root for which μ is always positive and which corresponds to the attachment line on the wing surface. We can use the expression for k given in equation (13) to examine the sign of the second root for μ, and from this we find that the second root is positive if and only if $\varepsilon>(3-\sqrt{5})/2$, which is precisely the condition given in equation (27) for an inboard flow separation to occur.

Therefore, as Smith[5] found for the thin-wing solution, the modification of the line-vortex model to deal with an inboard flow separation does not affect the leading terms for the vortex position and strength given by equations (16), (17) and (15a). The corresponding approximation for the position of separation will be

$$\chi=s+d(-\sin\varepsilon\pi+i\cos\varepsilon\pi)\frac{\mu^{1+2\varepsilon}}{1+2\varepsilon} \quad , \tag{35}$$

where

$$\mu=\frac{a}{2B_0}(\varepsilon k^2-1-\sqrt{1+\varepsilon(2-\varepsilon)k^2}) \quad . \tag{36}$$

For the thin-wing solution it is found that the position of separation moves inboard from the leading edges as the incidence increases from zero and then returns to the leading edge at about $a=0{\cdot}2$. Its maximum distance from the leading edge is less than 1 per cent of the semi-span. Introducing numerical values into equations (35) and (36) shows that the effect of increasing thickness is to reduce the inboard movement of the separation line.

2.4 Uniformly Valid Expansion

It was pointed out in Subsection 2.2 that the asymptotic expansion found is not uniformly valid in the limit $\varepsilon \to \frac{1}{2}$. Further examination of equation (12) shows that another change in behaviour of the solution arises in the limit as $\varepsilon \to 0$.

When the possibilities that ε may be close to 0 or $\frac{1}{2}$ (measured in terms of the small parameter a) are admitted, it becomes clear that other terms in (12) may become of the same order as those retained in deriving the solution (13). In particular when ε is small, the term

$$\frac{2d}{(1+2\varepsilon)s}(\sigma^2+\tau^2)^{2\varepsilon}(\sigma-i\tau) \tag{37}$$

must be retained. Also as ε approaches $\frac{1}{2}$, the leading terms which were retained for the expansion become smaller and so some of the higher order terms have to be retained. From the thin-wing results we require that $\sigma \sim (a/4)^{2/3}$, $\tau \sim (a/4)^{1/3}$ when $\varepsilon = \frac{1}{2}$ and we can in fact show that it is sufficient to include the term given by (37) along with the leading terms to ensure that the solution has the correct behaviour in this limit.

It is no longer possible to obtain an expansion in powers of a, but if we introduce the parameter P defined by

$$P = \frac{2d}{B_0 s}\frac{(\sigma^2+\tau^2)^{2\varepsilon}}{1+2\varepsilon} \tag{38}$$

then the revised equation can be written as

$$\frac{ia}{4B_0\sigma^2}(3\sigma^2-\tau^2-2\varepsilon\sigma(\sigma-i\tau)) = -(\sigma+i\tau)-P(\sigma-i\tau) \quad . \tag{39}$$

Equation (39) can now be solved to give σ and τ in terms of a and P, which can then be substituted into equation (38) to give

$$a = \frac{B_0}{\varepsilon}(1-2\varepsilon+(1+2\varepsilon)P)\left(\frac{1+P}{(3-2\varepsilon)(1-\varepsilon+P)}\right)^{1/2}\left(\frac{B_0 sP(1+2\varepsilon)}{2d}\right)^{1/4\varepsilon} \tag{40}$$

which, for a given value of a, can be used as an implicit equation to determine P. In terms of this parameter the solution can be written as

$$\sigma = \frac{a\varepsilon}{2B_0}\left(\frac{3-2\varepsilon}{1-2\varepsilon+(1+2\varepsilon)P}\right)^{1/2}\frac{1}{(1+P)^{1/2}} \quad , \tag{41a}$$

$$\tau = \frac{a\varepsilon}{2B_0}\frac{3-2\varepsilon}{1-2\varepsilon+(1+2\varepsilon)P} \quad , \tag{41b}$$

$$(Z_v - s)/s = \frac{d}{s(1+2\varepsilon)}\left(\frac{a\varepsilon}{2B_0}\left(\frac{3-2\varepsilon}{1-2\varepsilon+(1+2\varepsilon)P}\right)^{1/2}\left(\frac{1}{(1+P)^{1/2}}+i\left(\frac{3-2\varepsilon}{1-2\varepsilon+(1+2\varepsilon)P}\right)^{1/2}\right)\right)^{1+2\varepsilon} \quad , \tag{42}$$

and

$$\frac{C_L}{\alpha K} = 4\left(\frac{\pi\varepsilon d^2}{s^2}-\cot\varepsilon\pi\right)+\frac{4\pi d^2}{s^2}\left(\frac{(1+2\varepsilon)B_0 sP}{2d}\right)^{1/2\varepsilon} \quad . \tag{43}$$

This solution reduces to the previous solution when $1-2\varepsilon$ is not small, since $P \ll 1$ and $(1+2\varepsilon)P \ll 1-2\varepsilon$, and the terms involving P in equations (41) can be neglected. In the limit as $\varepsilon \to \frac{1}{2}$, P now becomes significant, and it can easily be checked that the thin wing result, $\sigma \sim (a/4)^{2/3}$, $\tau \sim (a/4)^{1/3}$ is recovered.

The lift coefficient given by equation (43) is plotted in Fig. 4 and shows very good agreement with the numerical solutions obtained in Ref. 6 using the vortex sheet model. Also plotted in this figure are the values predicted by equation (19), indicating the severely restricted range of values of a for which this expansion is applicable.

The vortex position given by equation (42) for $\varepsilon = 1/6$ is plotted in Fig. 3 along with the values for higher angles of incidence derived by Smith[6] using the vortex-sheet model. A direct comparison here is not possible however since, as pointed out in Subsection 2.2, the numerical solutions display an unexplained inboard deviation as the incidence decreases.

3. The Half-Circular Cone

This section, like the last, deals with a thick conical wing but in this case the wing is conically cambered to provide semi-circular cross-sections, so that the wing consists of one half of a circular cone. For consistency with earlier work[8], the flat surface of the cone is assumed to be uppermost and the angle of incidence α is defined as the angle between this surface and the free stream as shown in Fig. 5. This is drawn for a positive angle of incidence, for which fairly strong vortices will form over the flat surface of the wing. As the angle of incidence is reduced to negative values, the strength of these vortices is reduced until at one particular value, known as the attachment incidence, the flow remains attached. As the incidence is further reduced, vortices of the opposite sense are formed lying adjacent to the curved surface of the wing, and for incidences close to the attachment incidence the strength of the isolated vortices predicted by the Brown and Michael[1] model will be small. Asymptotic expansions for the strength and position of these vortices can therefore be found in terms of an incidence parameter related to the difference between the actual incidence and the attachment incidence.

In Ref. 8 Portnoy obtained the solution for the attached flow past a thin slender wing with a half-body of revolution mounted beneath it. The conformal transformation and the attached-flow solution for the present body therefore follow immediately by taking the semi-span of the wing to be equal to the body radius.

3.1 Formal Solution

This problem is solved by a method like that used for the rhombic cone, the main differences lying in the conformal transformation and the attached flow required to satisfy the wing boundary condition. The transformation, which is a special case of that given by Portnoy[8], is

$$\frac{Z+s}{Z-s} = -\left(\frac{\omega-1}{\omega+1}\right)^{3/2} ,$$

or

$$\frac{Z}{s} = \frac{(\omega^2-1)^{3/2}-\omega^3-3\omega}{3\omega^2+1} \tag{44}$$

and it maps the region external to the wing cross-section in the Z-plane onto the upper half of the ω-plane with the leading edges, $Z = \pm s$ being transformed into $\omega = \mp 1$ as shown in Fig. 6.

If we write

$$\omega = -1+\rho_1 \, e^{i\theta_1}$$

and

$$\omega = 1+\rho_2 \, e^{i\theta_2} \tag{45}$$

and restrict ω to lie on the Riemann sheet for which $0 \leq \theta_i \leq \pi$ $(i = 1, 2)$, then the fractional powers involved in equation (44) will be single-valued functions, and we can easily check that the boundary $BADCB$ in the ω-plane is correctly transformed into the wing cross-section shown in Fig. 6a. It should be noted that the point at infinity in the Z-plane is transformed by equation (44) into the point $i\sqrt{3}/3$ in the ω-plane.

From equation (44) we can show that

$$\frac{dZ}{d\omega} = \frac{3s\sqrt{\omega^2-1}}{\omega^3+3\omega+(\omega^2-1)^{3/2}} \, . \tag{46}$$

As in the previous section we can write down the complex conjugate velocity in the transformed plane as the attached flow terms which follow from Ref. 8 plus contributions due to vortices of equal and opposite strength $\pm\Gamma$ at the points ω_v and $-\bar{\omega}_v$. It is also necessary to introduce two image vortices in the lower half of the ω-plane to avoid disturbing the normal velocity condition on the wing boundary. With the angle of incidence of the plane upper surface of the wing measured in the direction shown in Fig. 5, the non-dimensional parameters a and γ are defined by

$$a = \alpha/K$$

and

$$\gamma = \Gamma/KUs \quad . \tag{47}$$

The complex conjugate velocity in the ω-plane is now given by

$$\frac{1}{KUs}\frac{dW}{d\omega} = \frac{32a\omega}{\sqrt{3}(3\omega^2+1)^2} + 3\frac{\omega-\sqrt{\omega^2-1}}{3\omega^2+1} + \frac{\gamma\omega}{\pi i}\left(\frac{1}{\omega^2-\omega_v^2} - \frac{1}{\omega^2-\bar{\omega}_v^2}\right) \quad , \tag{48}$$

where $\omega = \omega_v$ gives the position of the vortex in the first quadrant of the ω-plane. The first two terms in this expression represent the attached flow velocity given by Ref. 8 and the remaining terms are due to the four vortices combined in pairs. As before, the unknown quantities γ and ω_v are to be determined by the conditions that the velocity in the Z-plane should be finite at the leading edge and that the force acting on the right-hand vortex plus the cut joining it to the leading edge should be zero.

Since $dZ/d\omega$ vanishes at the leading edge, $\omega = -1$, the finite velocity condition requires that $dW/d\omega = 0$ at $\omega = -1$ and this condition can be expressed as

$$\gamma = -\frac{2\pi i(a-a_0)}{\sqrt{3}}\frac{(1-\omega_v^2)(1-\bar{\omega}_v^2)}{\omega_v^2-\bar{\omega}_v^2} \quad , \tag{49}$$

where $a_0 = -(3\sqrt{3}/8)$ and is the value of the incidence parameter for which the flow remains attached. The zero-force condition will take the same form as for the rhombic wing, that is

$$\lim_{Z\to Z_v}\left(\frac{dW}{dZ} - \frac{\Gamma}{2\pi i}\frac{1}{Z-Z_v}\right) = \frac{KU}{s}(2\bar{Z}_v - s) \quad . \tag{50}$$

Using equation (48) and noting that the only term in dW/dZ which is singular as $Z \to Z_v$ is that involving $1/(\omega-\omega_v)$ we can write equation (50) as

$$\frac{32a\omega_v}{\sqrt{3}(3\omega_v^2+1)^2} + 3\frac{\omega_v-\sqrt{\omega_v^2-1}}{3\omega_v^2+1} + \frac{\gamma}{2\pi i}\left(\frac{1}{2\omega_v} - \frac{2\omega_v}{\omega_v^2-\bar{\omega}_v^2} + \lim_{Z\to Z_v}\left(\frac{1}{\omega-\omega_v} - \frac{dZ}{d\omega}\frac{1}{Z-Z_v}\right)\right) = \frac{1}{s}\left(2\frac{\bar{Z}_v}{s} - 1\right)\left.\frac{dZ}{d\omega}\right|_{\omega=\omega_v} \quad . \tag{51}$$

The limit in this expression is obtained by expanding $Z - Z_v$ in a Taylor series about $\omega = \omega_v$ so that, after some manipulation, equation (51) becomes

$$\frac{32a\omega_v}{\sqrt{3}(3\omega_v^2+1)^2} + 3\frac{\omega_v-\sqrt{\omega_v^2-1}}{3\omega_v^2+1} - \frac{\gamma}{2\pi i}\left(\frac{1}{2\omega_v(\omega_v^2-1)} + \frac{2\omega_v}{\omega_v^2-\bar{\omega}_v^2} - \frac{3}{2(2\omega_v-\sqrt{\omega_v^2-1})}\right) = \left(2\frac{\bar{Z}_v}{s} - 1\right)\frac{1}{s}\left.\frac{dZ}{d\omega}\right|_{\omega=\omega_v} \quad , \tag{52}$$

and this equation, together with (49), will be sufficient to determine the vortex strength and position.

It is convenient to rearrange equation (52) to obtain

$$\frac{32(a-a_0)\omega_v}{\sqrt{3}(3\omega_v^2+1)^2}+\frac{3\sqrt{\omega_v^2-1}}{(3\omega_v^2+1)^2}((\omega_v^2+3\omega_v-1)\sqrt{\omega_v^2-1}-(\omega_v+1)^3)$$
$$-\frac{\gamma}{2\pi i}\left(\frac{1}{2\omega_v(\omega_v^2-1)}+\frac{2\omega_v}{\omega_v^2-\bar{\omega}_v^2}-\frac{3}{2(2\omega_v-\sqrt{\omega_v^2-1})}\right)=2\left(\frac{\bar{Z}_v}{s}-1\right)\frac{1}{s}\frac{dZ}{d\omega}\bigg|_{\omega=\omega_v}, \tag{53}$$

and it is in this form that the equation will be used subsequently.

3.2. Asymptotic Expansion for Small Vortex Strength

To find an approximate small vortex solution for this wing it is necessary to examine equations (49) and (53) at angles of incidence close to the attachment incidence. We therefore introduce the new incidence parameter p defined by

$$p=(a-a_0)/\sqrt{3} \quad , \tag{54}$$

and we look for an asymptotic solution to the problem in which $\omega_v \to -1$ as $p \to 0$. Accordingly we write

$$\omega_v = -1+\eta$$

and

$$\eta = \sigma + i\tau \tag{55}$$

and note that in accordance with equation (45) we must have $0 \leq \arg \eta \leq \pi$. If we make the assumption that τ is of the same order as σ and write $\tau = k\sigma$ in equation (49) we find that

$$\gamma = \frac{2\pi p\sigma(1+k^2)}{k}(1+O(\sigma^2)) \quad . \tag{56}$$

Inserting this into equation (53), making use of equations (44) and (46) and retaining only the first order terms, we obtain

$$-2p+\frac{9}{8}\sigma(1+ik)-\frac{p\sigma(1+k^2)}{ik}\left(\frac{1-ik}{4\sigma(1+k^2)}+\frac{1}{2k\sigma i}\right)=0 \quad . \tag{57}$$

Rearranging this equation and equating real and imaginary parts leads to

$$\frac{9}{8}\sigma = \frac{5k^2-2}{4k^2}p$$

and

$$\frac{9}{8}k\sigma = -\frac{p}{4k} \tag{58}$$

from which we find that $k = \mp(1/\sqrt{5})$ corresponding to

$$\eta = \frac{10}{9}p\left(-1\pm\frac{i}{\sqrt{5}}\right) \quad . \tag{59}$$

Now, since $0 < \arg \eta < \pi$, it follows that the imaginary part of η must be positive, and so we must choose the positive sign in equation (59) if p is positive and the opposite sign for negative p, with the different forms for the

solution corresponding to the vortices forming adjacent to the plane surface and the curved surface respectively. It should be noted that, with the plane surface of the wing uppermost, the lift on the wing at the attachment incidence will act in the downwards direction. Therefore the magnitude of the lift will increase as p becomes negative.

The leading terms in the expansion for the vortex position in the physical plane now follow from equations (44) and (59)

$$Z_v = s\left(1+\frac{2}{27}30^{3/4}|p|^{3/2}\exp\left(i\left(\frac{\pi}{4}\pm\frac{3}{2}\beta\right)\right)\right) \tag{60}$$

where $\tan\beta=\sqrt{5}$, $0<\beta<\pi/2$, and as before the positive sign corresponds to positive p. The vortex strength now follows from equations (56) and (59):

$$\gamma=\frac{8\pi\sqrt{5}}{3}p|p| \quad . \tag{61}$$

The corresponding approximation for the lift coefficient acting on the wing is derived in Appendix B and can be written as

$$\begin{aligned}\frac{C_L}{K^2} &= \frac{13\pi}{8\sqrt{3}}-4+\frac{19\pi}{3\sqrt{3}}p+\frac{640\pi}{27\sqrt{3}}p^3 \\ &= -1{\cdot}05+6{\cdot}63(a-a_0)+8{\cdot}27(a-a_0)^3 \quad .\end{aligned} \tag{62}$$

The first two terms in this expression give the attached flow contribution to the lift and are a special case of the result given by Portnoy[8], and the remaining term is the non-linear contribution due to the vortices above the wing.

To this first approximation, the magnitudes of both the vortex strength and the non-linear lift are the same for the same increment in incidence either above or below the attachment incidence. There seems to be no physical reason to expect this result, since the vortex lies alongside the curved surface of the half-cone for angles of incidence above the attachment incidence and adjacent to the flat surface for angles of incidence below it.

This result for the lift of the half-circular cone can be compared with that for the rhombic cone of the same edge angle by setting $\varepsilon = 0{\cdot}25$ in equation (19):

$$\frac{C_L}{K^2}=4{\cdot}75a+28{\cdot}2a^3 \quad .$$

Comparing the two wings at the same incidence away from the attached flow condition, we see that the half-circular cone produces more linear lift, but less non-linear lift than the uncambered wing with the same edge angle. Too much reliance should not be placed on this comparison in view of the limited range of values of a for which (19) is an adequate representation of the lift.

Since the edge angle of 90 degrees for the half-circular cone is greater than the largest value for which inboard separation was found to occur for the rhombic cone considered in Section 2 we would expect to find that the flow near the leading edge is directed outboard across the conical rays, indicating that the separation does in fact occur from the leading edge. This point will now be confirmed.

Close to the leading edge $\omega = -1$ and we can approximate to ω using either of the expressions in equation (45) where ρ_1 will be small and θ_2 will be close to π. Substituting these approximations into equation (48) leads to

$$\begin{aligned}\frac{1}{KUs}\frac{dW}{d\omega} = &-2p-\frac{3}{4}(\rho_1\rho_2)^{1/2}\,e^{i(\theta_1+\theta_2)/2}-\left(4p-\frac{9}{8}\right)\rho_1\,e^{i\theta_1} \\ &-\frac{\gamma(\omega_v^2-\bar{\omega}_v^2)}{\pi i(1-\omega_v^2)(1-\bar{\omega}_v^2)}\left(1+\rho_1\,e^{i\theta_1}\left(\frac{2(2-\omega_v^2-\bar{\omega}_v^2)}{(1-\omega_v^2)(1-\bar{\omega}_v^2)}-1\right)\right)+O(\rho_1^{3/2}) \quad .\end{aligned} \tag{63}$$

Using equation (49) for the vortex strength, and equations (55) and (59) to approximate its position we find that equation (63) reduces to

$$\frac{1}{KUs}\frac{dW}{d\omega}=-\frac{3}{4}(\rho_1\rho_2)^{1/2}\,e^{i(\theta_1+\theta_2)/2}\left(1+\frac{4}{3}\left(\frac{\rho_1}{\rho_2}\right)^{1/2}e^{i(\theta_1-\theta_2)/2}\left(\frac{15}{8}+O(p)\right)+O(\rho_1)\right) \tag{64}$$

from which, with the aid of equation (46), the complex conjugate velocity near the leading edge is given by

$$\frac{1}{KU}\frac{dW}{dZ}=1+\frac{4}{3}\left(\frac{\rho_1}{\rho_2}\right)^{1/2}e^{i(\theta_1-\theta_2)/2}\left(\frac{15}{8}+O(p)\right)+O(\rho_1)\quad . \tag{65}$$

The first term on the right-hand side of this expression represents the velocity in the cross-flow plane at the leading edge, and so the second term approximates to the velocity relative to the leading edge. From Fig. 6 we can see that on the plane surface AB, $\theta_1=\theta_2=\pi$ and so the second term in equation (65) will be real and positive, indicating that the velocity relative to the leading edge is directed outboard. Also, on the curved surface AD, $\theta_1=0$ and $\theta_2=\pi$, so that the second term will represent a velocity which is upward and therefore directed towards the leading edge.

3.3 Comparison with Similarity Theory

The consistency of the leading terms given by equations (16) and (60) for the two different wing cross-sections can be checked with the aid of the similarity theory of Maskell first put forward in 1960[9]. This theory relates the development of small leading-edge vortex systems on wings of different cross-sections but with the same edge angle. The present account is based on unpublished work by Maskell extending Ref. 9.

If Z_1 is the complex coordinate based on the wing leading edge, with its real axis aligned along the bisector of the edge angle, then close to the leading edge the attached-flow contribution to the complex velocity potential can be expanded in the form

$$\frac{1}{KUs}W_a=-iA_1Z_1^{1/(2-n)}+\frac{Z}{s}+(A_2-A_0)Z_1^{2/(2-n)}+\ldots \tag{66}$$

where A_0, A_1 and A_2 are constants depending on the geometry of the wing cross-section and $n\pi$ is the edge angle. The term with coefficient A_0 is due to the flow at the attachment incidence, whereas the terms with coefficients A_1 and A_2 are due to the incidence and sideslip measured relative to this position, vanishing at the attachment incidence for zero sideslip.

Maskell's theory states that, for a small vortex system, the position and strength of corresponding points on the vortex sheet, or in this particular case the position and strength of the isolated vortex, can be written in the form

$$Z_1=Lf(n,P) \tag{67}$$

and

$$\frac{\Gamma}{KUs}=L^2g(n,P) \tag{68}$$

where L and P are non-dimensional similarity parameters defined in terms of A_0, A_1 and A_2. These length-scale and incidence parameters are proportional to $(A_0-A_2)^{[(2-n)/(2(1-n))]}$ and $A_1/(A_0-A_2)^{[(3-2n)/(2(1-n))]}$ respectively, and, for each value of n, the constants of proportionality are chosen so that they reduce to 1 and α/K respectively for the rhombic wing at zero sideslip.

The attached flow contributions to the velocity potential can be derived from equation (3) with the vortex contribution omitted. For comparison of this wing with the half-circular cone we are interested only in the case $\varepsilon=\frac{1}{4}$ for which the leading-edge angle is a right angle, so that we can expand equation (3) with the aid of equations (9), (10) and (2) and integrate to obtain

$$\frac{1}{KUs}W_a=-ia\frac{d}{s}\left(\frac{3s}{2d}Z_1\right)^{2/3}+\frac{Z}{s}-\frac{2}{\pi}\left(\frac{3s}{2d}Z_1\right)^{4/3}+O(Z_1^2)\quad , \tag{69}$$

the arbitrary constant having been omitted.

Comparison of equation (69) with (66) for $n=\frac{1}{2}$ indicates that, for the rhombic cone,

$$A_1=\left(\frac{3}{2}\right)^{2/3}\left(\frac{d}{s}\right)^{1/3}a \tag{70}$$

and

$$A_0-A_2=\frac{2}{\pi}\left(\frac{3s}{2d}\right)^{4/3} \tag{71}$$

so that the similarity parameters can be written as

$$L=\frac{\sqrt{2}d^2\pi^{3/2}}{9s^2}(A_0-A_2)^{3/2} \tag{72}$$

and

$$P=\frac{9s^3}{\pi^2d^3}\frac{A_1}{(A_0-A_2)^2} \quad . \tag{73}$$

For the rhombic cone, $Z_1=[(Z-s)/s]$, and so, for $\varepsilon=\frac{1}{4}$, the leading term in equation (16) gives

$$Z_1=\frac{2d}{3s}(p_{00}a)^{3/2} \tag{74}$$

where p_{00} is given by equation (15a). For $\varepsilon=\frac{1}{4}$, $k=\sqrt{5}$, and so in terms of the angle β defined by $\tan\beta=\sqrt{5}$, $0<\beta<\pi/2$, we find that

$$p_{00}=\frac{\pi d}{4s}\sqrt{\left(\frac{15}{32}\right)}\,e^{i\beta} \quad . \tag{75}$$

Since, for this wing, $L=1$ and $P=a$ comparison of equations (74) and (75) with equation (67) shows that

$$f(\tfrac{1}{2},P)=\left(\frac{15}{32}\right)^{3/4}\frac{\pi^{3/2}}{12}\left(\frac{d}{s}\right)^{5/2}P^{3/2}\,e^{3i\beta/2} \quad . \tag{76}$$

Similarly comparison of equations (17) and (75) with equation (68) yields

$$g(\tfrac{1}{2},P)=\frac{3\sqrt{5}}{16}\pi^2\left(\frac{d}{s}\right)^2P^2 \quad . \tag{77}$$

The attached-flow complex velocity potential for the half-circular cone can be obtained from equation (48) with $\gamma=0$. Making the substitution $\omega=-1+\eta$ and expanding for small $|\eta|$ we find

$$\frac{1}{KUs}\frac{dW_a}{d\eta}=-\frac{2}{\sqrt{3}}\left(a+\frac{3\sqrt{3}}{8}\right)-\frac{3i}{2\sqrt{2}}\eta^{1/2}-\left(\frac{4a}{\sqrt{3}}+\frac{3}{8}\right)\eta+O(\eta^{3/2}) \quad , \tag{78}$$

and so

$$\frac{1}{KUs}W_a=-\frac{2}{\sqrt{3}}\left(a+\frac{3\sqrt{3}}{8}\right)\eta-\frac{i}{\sqrt{2}}\eta^{3/2}-\frac{2}{\sqrt{3}}\left(a+\frac{3\sqrt{3}}{32}\right)\eta^2+O(\eta^{5/2}) \quad . \tag{79}$$

For this wing the complex coordinate Z_1 is defined by

$$Z_1 = \frac{Z-s}{s} e^{-\pi i/4} \quad , \tag{80}$$

and so applying this to equation (44) and making the approximation used above gives

$$\eta = 2i\left(\frac{Z_1}{2}\right)^{2/3}\left(1 - i\left(\frac{Z_1}{2}\right)^{2/3} + O(Z_1)\right) \tag{81}$$

and

$$Z = s(1 - \tfrac{1}{2}i\sqrt{2}\eta^{3/2} + O(\eta^{5/2})) \quad . \tag{82}$$

The complex potential can now be written

$$\frac{1}{KUs} W_a = -\frac{4}{\sqrt{3}} i\left(a + \frac{3\sqrt{3}}{8}\right)\left(\frac{Z_1}{2}\right)^{2/3} + \frac{Z}{s} + \frac{4}{\sqrt{3}}\left(\left(a + \frac{3\sqrt{3}}{8}\right) - \frac{9\sqrt{3}}{16}\right)\left(\frac{Z_1}{2}\right)^{4/3} + \ldots \quad , \tag{83}$$

where the arbitrary constant has been omitted.

Comparison of equations (66) and (83) now shows that

$$A_1 = \frac{2^{4/3}}{\sqrt{3}}\left(a + \frac{3\sqrt{3}}{8}\right) \tag{84}$$

and

$$A_0 - A_2 = \frac{2^{2/3}}{\sqrt{3}}\left(\frac{9\sqrt{3}}{16} - \left(a + \frac{3\sqrt{3}}{8}\right)\right) \quad . \tag{85}$$

As pointed out earlier in this subsection, A_2 is proportional to $(a + (3\sqrt{3}/8))$, which vanishes at the attachment incidence. In the present approximation this term is small compared with A_0 and so can be neglected. It is only when this term is retained that the similarity theory will predict different forms for the solution at incidences above and below attachment.

With this assumption we can substitute the expressions (84) and (85) into (72) and (73) to obtain the length-scale and incidence parameters for the half-circular cone:

$$L = \frac{3\sqrt{2}\pi^{3/2}d^2}{32s^2} \tag{86}$$

and

$$P = \frac{256s^3}{9\sqrt{3}\pi^2 d^3}\left(a + \frac{3\sqrt{3}}{8}\right) \quad . \tag{87}$$

It can now be checked that by combining these with equations (67) and (76), and with equations (68) and (77), the asymptotic expressions obtained agree with the vortex position and strength given by equations (60) and (61).

4. The Flat-Plate Wing

The wing considered is without thickness or warp, consisting of that part of the plane $z = 0$ for which $0 \leq x \leq c$ and $-s(x) \leq y \leq s(x)$. The local semi-span, $s(x)$, is a differentiable function of the coordinate x measured downstream along the centre line of the wing from the apex. It is assumed that $s'(0) > 0$, so that the

wing is asymptotic to a delta wing at its apex, and that $s'(x) \geq 0$ for $0 < x \leq c$. The aspect ratio

$$A = 2s^2(c) \Big/ \int_0^c s(x)dx \tag{88}$$

is small. This wing is at a uniform small angle of incidence, α, to the free stream of speed U.

The application of the line-vortex model of the flow to this configuration is described in Ref. 11, from which the equations governing the model will be extracted as required. The line vortex will be assumed to lie close to the leading edge, in such a way that its vertical and lateral displacements from the edge tend to zero like positive powers of α as the incidence tends to zero. The coefficients of these powers of α are functions of x, satisfying ordinary differential equations. Solutions of these equations are found in closed form in Sub-sections 4.1 to 4.4, providing asymptotic expressions, valid as α/A tends to zero, for the position and strength of the vortex, and the lift and pitching moment of the wing. Sub-section 4.5 presents a comparison with a numerical solution of the equations of Ref. 11, for a gothic wing, and an application to the analysis of experimental measurements is described in Sub-section 4.6.

4.1. The Equations

The circulation of the starboard vortex is represented by $\Gamma = \gamma Us$ and its position by $y = \eta s$ and $z = \zeta s$, where γ, η and ζ are non-dimensional functions of x to be determined. A conformal transformation is introduced which maps the cross-flow plane $x =$ constant outside the wing slit $|y| \leq s$, $z = 0$ on to a plane in which the slit lies in the vertical plane of symmetry. If the non-dimensional coordinates of the starboard vortex in this transformed plane are σ and τ, we have

and

$$\left.\begin{aligned} 1 - \eta^2 + \zeta^2 &= \tau^2 - \sigma^2 \\ \eta\zeta &= \sigma\tau \quad , \end{aligned}\right\} \tag{89}$$

by equation (I.1) of Ref. 11. The Kutta-Joukowski condition of finite velocity at the leading edge yields

$$\frac{\gamma}{2\pi\alpha} = \frac{\sigma^2 + \tau^2}{2\sigma} \quad , \tag{90}$$

which is (I.2) of Ref. 11; and the two equations which express the vanishing of the two components of the transverse force on the combination of the vortex and the cut joining it to the leading edge can be written as

$$s\eta' = F\alpha - (2\eta - 1)s' + s(1-\eta)\gamma'/\gamma \tag{91}$$

and

$$s\zeta' = G\alpha - 2\zeta s' - s\zeta\gamma'/\gamma \quad , \tag{92}$$

where primes denote derivatives with respect to x, and

$$\left.\begin{aligned} F &= \frac{1}{2\sigma(\sigma^2+\tau^2)}\left\{\frac{\zeta(\eta^2 - \frac{1}{2}(\tau^2-\sigma^2))}{\eta^2+\zeta^2} + \frac{(\eta\tau - \zeta\sigma)(\tau^2 - 3\sigma^2)}{2\sigma}\right\} \\ G &= \frac{1}{2\sigma(\sigma^2+\tau^2)}\left\{\frac{\eta(\zeta^2 + \frac{1}{2}(\tau^2-\sigma^2))}{\eta^2+\zeta^2} - \frac{(\eta\sigma + \zeta\tau)(\tau^2 - 3\sigma^2)}{2\sigma}\right\} \end{aligned}\right\} , \tag{93}$$

by equations (I.4) and (I.8) of Ref. 11. Finally, for the lift $L(x)$ acting on that part of the wing upstream of the station x, a momentum calculation yields

$$L(x) = \rho U^2 s^2(\pi\alpha + 2\gamma\sigma) \quad , \tag{94}$$

where ρ is the density, by equation (9) of Ref. 11. Here the first term is the result of R. T. Jones for the attached flow, and the second term represents the non-linear lift arising from the vortices.

Inspection of equations (91) and (92) suggests that the form of the asymptotic solution for small α (σ, τ, γ, ζ small, $\eta \sim 1$) may depend on whether $s'(x)$ is strictly positive or zero (planforms for which $s'(x)<0$ are excluded from consideration). This turns out to be the case. The solution for $s'(x)>0$ is found in the following sub-section. If $s'(x_0)=0$, this solution breaks down as $x \to x_0$ from below, with the coefficient of the leading term in the expansion increasing indefinitely. A coordinate stretching procedure, in the neighbourhood of $x=x_0$, is introduced in Sub-section 4.3, and provides a solution which can be matched to the upstream solution. If the wing continues downstream of $x=x_0$ further consideration is needed. This is given in Sub-section 4.4 for the special case of the wing with streamwise edges, i.e. $s(x)=s(x_0)$ for $x \geq x_0$.

4.2. Solution for $s'(x) > 0$

Since any solution found must embrace that for the delta wing, for which s' is constant, it is reasonable to seek a solution of the form found for the delta wing. Following Refs. 1 and 5, we introduce a small parameter t:

$$t=(\alpha/4)^{1/3} \quad , \tag{95}$$

and suppose that

$$\left.\begin{aligned} \sigma &= \sigma_0(x)t^2+O(t^3) \\ \tau &= \tau_0(x)t+O(t^2) \quad . \end{aligned}\right\} \tag{96}$$

It is then clear from equation (89) that

and

$$\left.\begin{aligned} \eta &= 1-\tfrac{1}{2}\tau_0^2 t^2+O(t^3) \\ \zeta &= \sigma_0\tau_0 t^3+O(t^4) \quad . \end{aligned}\right\} \tag{97}$$

Equations (90) and (96) now give

$$\frac{\gamma'}{\gamma}=\frac{\sigma_0}{\tau_0^2}\left(\frac{\tau_0^2}{\sigma_0}\right)'+O(t) \quad . \tag{98}$$

The leading term in F is found easily:

$$F=\frac{\tau_0}{4\sigma_0^2 t^3}+O\left(\frac{1}{t^2}\right) \tag{99}$$

and a little manipulation produces

$$G=\frac{\sigma_0}{2\tau_0^2}+O(t) \quad . \tag{100}$$

It is now clear that equation (91) is dominated by the first two terms on the right, which are $O(1)$. Equating them gives

$$\tau_0=\sigma_0^2 s' \quad . \tag{101}$$

All the terms in equation (92) are $O(t^3)$; equating them and rearranging the result gives

$$\left(\tau_0^3 s^2\right)'=2s \quad .$$

This can be integrated directly to give

$$\tau_0^3 s^2 = S(x)=2\int_0^x s(\xi)d\xi \quad , \tag{102}$$

since τ_0 must be finite at $x=s=0$ to match the known solution for a delta wing. $S(x)$ is just the planform area

upstream of the plane $x =$ constant. It is convenient to introduce a 'local aspect ratio',

$$A(x) = 4s^2(x)/S(x) \quad , \tag{103}$$

noting that $A(c) = A$.

The leading terms in the asymptotic expansion of the solution can now be expressed in terms of $s(x)$, $s'(x)$, $A(x)$ and α. For the non-dimensional vortex position, from equations (95), (97), (101), (102) and (103):

$$\eta = 1 - \frac{1}{2}\left(\frac{\alpha}{A(x)}\right)^{2/3} + O(\alpha) \tag{104}$$

and

$$\zeta = \frac{\alpha}{2(A(x)s'(x))^{1/2}} + O(\alpha^{4/3}) \quad . \tag{105}$$

The vortex strength follows from equations (90), (96), (101), (102) and (103):

$$\Gamma = \gamma U s = 2\pi\alpha U s(x)\left(\frac{s'(x)}{A(x)}\right)^{1/2} + O(\alpha^{4/3}) \quad , \tag{106}$$

and the lift acting forward of the station x is given by equation (94):

$$L(x) = \pi\rho U^2 \alpha s^2(x)\left(1 + 2\left(\frac{\alpha}{A(x)}\right)^{2/3} + O(\alpha)\right) \quad . \tag{107}$$

These expressions agree with those of Refs. 1 and 5 in the case of a delta wing, for which $s'(x)$ and $A(x)$ are constant. It is of some interest to recall a conjecture made in Ref. 11, on the basis of numerical solutions of equations (91) and (92), that $C_L/\alpha A$ (which is equal to $L/2\rho U^2 \alpha s^2$) might be a function of α/A only, independent of the actual planform shape. Equation (107) confirms that this is so for small values of α/A, and Fig. 6 of Ref. 11 shows that the evidence for the conjecture is strongest for small values of α/A.

The solution obtained is valid (for small enough values of α) provided $s'(x) > 0$. As $s'(x)$ tends to zero the solution breaks down, as indicated by the right-hand side of equation (105) tending to infinity. The explanation is that $s'(x)$ appears in the leading terms of equations (91) and (92). To obtain a meaningful solution for $s'(x)$ small, it is necessary to relate the magnitudes of $s'(x)$ and α, and this is now attempted through a stretching of the x coordinate.

4.3. Extension of the Solution to the Station at which $s'(x) = 0$

Consider a planform for which $s'(x) > 0$ for $x < x_0$ and $s'(x_0) = 0$. To examine the behaviour of the governing equations for small α and small $x_0 - x$, we introduce a stretched coordinate ξ defined by

$$x = x_0 - t^m \xi \tag{108}$$

where $m > 0$ is to be chosen in such a way that a solution is obtained, and t is given by equation (95). Retaining the form of equation (96) for σ and τ does not lead to a solution which can be matched satisfactorily to the upstream solution of the previous sub-section. On the other hand, (102) defines a well-behaved function $\tau_0(x)$, so it is reasonable to retain the form for τ, and try for an inner solution of the form

$$\sigma = \sigma_1(\xi)t^n + \ldots \quad , \qquad \tau = \tau_1(\xi)t + \ldots \quad . \tag{109}$$

It emerges that $1 < n < 2$, and this will be assumed in order to simplify the presentation.

It follows at once from equations (89) that

$$\left.\begin{aligned} \eta &= 1 - \tfrac{1}{2}\tau_1^2 t^2 + \tfrac{1}{2}\sigma_1^2 t^{2n} + \ldots \\ \zeta &= \sigma_1 \tau_1 t^{n+1} + \ldots \quad , \end{aligned}\right\} \tag{110}$$

and

and equations (93) become

$$F=\frac{\tau_1}{4\sigma_1^2 t^{2n-1}}+\ldots \quad \text{and} \quad G=\frac{\sigma_1}{2\tau_1^2 t^{2-n}}+\ldots \quad . \tag{111}$$

From equation (108), $dx/d\xi=-t^m$, and so, by equation (110):

$$\eta'=d\eta/dx=\tau_1\tau_1' t^{2-m}-\sigma_1\sigma_1' t^{2n-m}+\ldots$$

and

$$\zeta'=d\zeta/dx=-(\sigma_1\tau_1)' t^{n-m+1}+\ldots \quad ,$$

where, on the right-hand side, primes denote differentiation with respect to ξ. Similarly, from equations (90) and (109),

$$\frac{\gamma'}{\gamma}=\frac{1}{\gamma}\frac{d\gamma}{dx}=-\frac{\sigma_1}{t^m\tau_1^2}\left(\frac{\tau_1^2}{\sigma_1}\right)'+\ldots \quad .$$

The equation of the leading edge immediately upstream of $x=x_0$ can be expanded as

$$y=s(x)=s(x_0)-B(x_0-x)^l+\ldots \tag{112}$$

where $l>1$ and B is a positive constant. Hence

$$s'(x)=Bl(x_0-x)^{l-1}+\ldots=Blt^{lm-m}\xi^{l-1}+\ldots \quad , \tag{113}$$

by equation (108). With these expressions, the leading terms in equations (91) and (92) can be written as:

$$s_0\tau_1\tau_1' t^{2-m}-s_0\sigma_1\sigma_1' t^{2n-m}=\tau_1 t^{4-2n}/\sigma_1^2-Blt^{lm-m}\xi^{l-1}-\tfrac{1}{2}s_0\sigma_1 t^{2-m}(\tau_1^2/\sigma_1)'+\ldots \tag{114}$$

$$-s_0(\sigma_1\tau_1)' t^{n+1-m}=2\sigma_1 t^{n+1}/\tau_1^2-2\sigma_1\tau_1 Blt^{n+1-m+lm}\xi^{l-1}+s_0\sigma_1^2(\tau_1^2/\sigma_1)' t^{n+1-m}/\tau_1+\ldots \quad , \tag{115}$$

where $s_0=s(x_0)$.

In equation (115) the first two terms on the right are of higher order than the others, since $m>0$ and $l>0$. Equating the lower order terms gives

$$\frac{(\sigma_1\tau_1)'}{\sigma_1\tau_1}+\frac{\sigma_1}{\tau_1^2}\left(\frac{\tau_1^2}{\sigma_1}\right)'=0 \quad ,$$

which is directly integrable to give $\tau_1=$ constant. The value of the constant is obtained by matching this inner solution to the outer solution (102). The process leads trivially to

$$\tau_1(\xi)=\tau_0(x_0)=(4/A(x_0))^{1/3} \quad . \tag{116}$$

Since $\tau_1'=0$, it is now clear why an additional term has been retained in the expansion of η'. However, inspection of equation (114) shows that the second term on the left is of higher order than the last term on the right. The three terms on the right can be combined in four different ways. Omitting the first leads to an expression for σ_1 which grows exponentially as ξ increases. This cannot be matched to the outer solution. Omitting the second leads to an expression for σ_1^2 which becomes negative as ξ increases, and again cannot be matched. Omitting the third leads to an expression for σ_1 which is unbounded as $\xi\to 0$ and affords no improvement over the outer solution. With all four of the same order:

$$4-2n=lm-m=2-m$$

and

$$s_0\sigma_1(\tau_1^2/\sigma_1)'+2Bl\xi^{l-1}-2\tau_1/\sigma_1^2=0 \quad .$$

Hence

$$m=2/l \quad \text{and} \quad n=1+1/l \quad . \tag{117}$$

With $\tau_1'=0$ and the substitution $\sigma_1^2=f(\xi)$, the differential equation becomes linear:

$$f'-\lambda^2 l\xi^{l-1}f+4/s_0\tau_1=0 \quad , \tag{118}$$

where $\lambda^2=4B/s_0\tau_1^2>0$. The solution can be obtained, using an integrating factor, as

$$\sigma_1^2=f=\exp(\lambda^2\xi^l)\left\{C-\frac{4}{s_0\tau_1}\int_0^{\xi}\exp(-\lambda^2u^l)du\right\} \quad ,$$

where C is a constant and u is a dummy variable of integration. C should be determined by matching to the outer solution. In fact, its value is obtained without recourse to the formal procedure, since it is a prerequisite that σ_1 is bounded as $\xi\to\infty$. Hence

$$C=\frac{4}{s_0\tau_1}\int_0^{\infty}\exp(-\lambda^2u^l)du$$

and

$$\sigma_1^2=\frac{4}{s_0\tau_1}\exp(\lambda^2\xi^l)\int_{\xi}^{\infty}\exp(-\lambda^2u^l)du \quad . \tag{119}$$

The integral can be expressed as an incomplete gamma function, by for example 8.350.2 of Ref. 15:

$$\sigma_1^2=\frac{4\exp(\lambda^2\xi^l)}{s_0\tau_1 l\lambda^{2/l}}\Gamma\left(\frac{1}{l},\lambda^2\xi^l\right) \quad . \tag{120}$$

The asymptotic expansion of Γ for large values of ξ, from 8.357 of Ref. 15, gives

$$\sigma_1^2=\frac{4}{s_0\tau_1\lambda^2 l\xi^{l-1}}\left(1-\frac{l-1}{\lambda^2 l\xi^l}+0(\xi^{-2l})\right) \quad . \tag{121}$$

We can now verify that this inner solution (119) matches the outer solution. The first step is to express it in terms of the outer variable x. ξ is given by equation (108) and so

$$\xi^l=(x_0-x)^l/t^2 \quad , \qquad \text{using equation (117).}$$

Therefore, for small values of t, ξ is large, and we need only look at the leading term of equation (121). Using this leading term, with equations (117) and (118), we find from equation (109) the single-term outer expansion of the single-term inner solution as:

$$\sigma=\sigma_1 t^n+\ldots=\sqrt{\frac{\tau_1}{Bl(x_0-x)^{l-1}}}t^2+\ldots \quad . \tag{122}$$

According to the matching principle of Van Dyke[16] this should be the same as the single-term inner expansion of the single-term outer solution. The outer solution, by equations (96) and (101), is

$$\sigma=\sqrt{\frac{\tau_0}{s'(x)}}t^2+\ldots \quad .$$

If we write this in terms of x_0-x, by equations (108) and (113), and take the leading term for small values of t, we do indeed recover solution (122).

The next step is to form a composite expansion[16] or other expression for σ valid over the whole range $0 \leq x \leq x_0$. It is perhaps more revealing to look at the process for a particular planform. Consider the gothic wing of unit chord and aspect ratio A, for which

$$s(x) = Ax(2-x)/3 \quad \text{for} \quad 0 \leq x \leq x_0 = 1 \quad . \tag{123}$$

Then $s'(x) = 2A(1-x)/3$ and, by equations (102) and (103),

$$A(x) = 2A(2-x)^2/(3-x) \quad .$$

The outer solution, (104) to (107), is then

$$\left.\begin{aligned} \eta &= 1 - \frac{1}{2}\left(\frac{\alpha}{A}\frac{3-x}{2(2-x)^2}\right)^{2/3} + \ldots \quad , \\ \zeta &= \frac{\alpha}{A}\frac{\sqrt{3(3-x)}}{4(2-x)\sqrt{1-x}} + \ldots \quad , \\ \frac{\Gamma}{A^2} &= 2\pi U \frac{\alpha}{A}\frac{x}{3}\sqrt{\frac{(1-x)(3-x)}{3}} + \ldots \\ \text{and} \qquad L(x) &= \pi\rho U^2 \alpha s^2(x)\left(1 + 2\left(\frac{\alpha}{A}\frac{3-x}{2(2-x)^2}\right)^{2/3} + \ldots\right) \quad . \end{aligned}\right\} \tag{124}$$

The similarity parameter α/A is now apparent, as is the breakdown of the outer solution for ζ and Γ as $x \to 1$. To supplement this the inner solution is required. Comparing equations (123) and (112), we find $l = 2$ and $B = A/3$. Hence by equations (116) to (118):

$$\tau_1 = (4/A)^{1/3} \quad , \qquad m = 1 \quad , \qquad n = 3/2 \quad \text{and} \quad \lambda = 2(A/4)^{1/3} \quad .$$

The expression (119) can best be written in terms of

$$\bar{\xi} = \lambda\xi = \lambda(1-x)/t = 2(A/\alpha)^{1/3}(1-x) \quad . \tag{125}$$

It becomes $\sigma_1^2 = 6g(\bar{\xi})/A$, where

$$g(\bar{\xi}) = \exp(\bar{\xi}^2)\int_{\bar{\xi}}^{\infty} \exp(-u^2)du = \frac{\sqrt{\pi}}{2}\exp(\bar{\xi}^2)\,\mathrm{erfc}(\bar{\xi}) \quad , \tag{126}$$

in terms of the complementary error function. The inner solution for ζ follows from equations (110):

$$\zeta = \left(\frac{3g(\bar{\xi})}{2}\right)^{1/2}\left(\frac{\alpha}{A}\right)^{5/6} + \ldots \quad . \tag{127}$$

The corresponding inner solution for the vortex strength Γ follows in the same way:

$$\frac{\Gamma}{A^2} = \frac{\pi U}{3}\sqrt{\frac{2}{3g(\bar{\xi})}}\left(\frac{\alpha}{A}\right)^{7/6} + \ldots \quad . \tag{128}$$

The significance of the variable $\bar{\xi}$, equation (125), is apparent when it is remembered that the entire expansion procedure is for small values of α/A. When $x = 1$, $\bar{\xi} = 0$; when $1-x$ is small, of order $(\alpha/A)^{1/3}$, $\bar{\xi}$ takes values which are of order one; and when $1-x$ is of lower order, $\bar{\xi}$ becomes large. Now $g(0) = \sqrt{\pi}/2$, finite, while $g(\bar{\xi}) \to 0$ as $\bar{\xi} \to \infty$. The leading term in ζ in the outer solution is $0(\alpha/A)$, with a coefficient which tends to infinity as $x \to 1$. In the inner solution this is replaced by a term of lower order, $(\alpha/A)^{5/6}$, whose coefficient tends to zero as $\bar{\xi} \to \infty$. The leading term in Γ behaves in the opposite fashion: in the outer solution

the leading term, again $0(\alpha/A)$, has a coefficient which vanishes at $x=1$; while the leading term in the inner solution is of higher order and its coefficient tends to infinity as $\bar{\xi}\to\infty$.

It is convenient to have single expressions for ζ and Γ, valid over the whole range $0\leqslant x\leqslant 1$. These can be formed as composite expansions[16], adding the inner and outer solutions and subtracting from the sum their 'common part', the inner expansion of the outer solution (equal to the outer expansion of the inner solution). Carrying out the inner expansion of the outer solutions (124) for ζ and Γ, and returing to the outer variable x, we find

$$\zeta=\frac{1}{2}\sqrt{\frac{3}{2(1-x)}}\frac{\alpha}{A}+\ldots$$

and

$$\frac{\Gamma}{A^2}=\frac{2\pi U}{3}\sqrt{\frac{2(1-x)}{3}}\frac{\alpha}{A}+\ldots\ .$$

The composite expansions follow by subtracting these from the sums of (124) and (127) or (128):

$$\zeta_{\text{comp}}=\sqrt{\frac{3g(\bar{\xi})}{2}}\left(\frac{\alpha}{A}\right)^{5/6}-\frac{1}{4}\sqrt{\frac{3}{1-x}}\left(\sqrt{2}-\frac{\sqrt{3-x}}{2-x}\right)\frac{\alpha}{A}+\ldots \tag{129}$$

$$\left(\frac{\Gamma}{A^2}\right)_{\text{comp}}=-\frac{2\pi U}{3}\sqrt{\frac{1-x}{3}}(\sqrt{2}-x\sqrt{3-x})\frac{\alpha}{A}+\frac{\pi U}{3}\sqrt{\frac{2}{3g(\bar{\xi})}}\left(\frac{\alpha}{A}\right)^{7/6}+\ldots\ . \tag{130}$$

When $x\to 1$ and $\bar{\xi}\to 0$, these expressions agree with the inner solutions (127) and (128). In the limit $\bar{\xi}\to\infty$, they agree with the outer solutions (124). How appropriate the limit $\bar{\xi}\to\infty$ is at a particular value of $x<1$ depends on the size of α/A, through (125).

The numerical behaviour of these solutions is discussed in Sub-section 4.5.

4.4 Solution for Wing with Side-Edges

For a portion of a slender wing with streamwise edges, $s(x)=s(x_0)$ for $x\geqslant x_0$, we have $s'(x)=0$ and the differential equations (91) and (92) reduce to:

$$\left.\begin{aligned} s\eta' &= F\alpha+s(1-\eta)\gamma'/\gamma \\ s\zeta' &= G\alpha-s\zeta\gamma'/\gamma\ . \end{aligned}\right\} \tag{131}$$

After some experimentation it was concluded that a solution to these equations for small angles of incidence only existed if σ and τ were both of order $t=(\alpha/4)^{1/3}$. Since we are assuming that $s'(x)$ is continuous and non-negative, upstream of $x=x_0$ the solution of the previous sub-sections must apply. In this, the leading term in σ at $x=x_0$ is $0(t^n)$, where n depends on the shape of the edge in the neighbourhood of $x=x_0$, but is strictly between 1 and 2. The order of the leading term must therefore be expected to change at $x=x_0$.

The necessary degree of generality is obtained by setting

and

$$\left.\begin{aligned} \sigma &= t\sigma_2(x,t)+0(t^2) \\ \tau &= t\tau_2(x,t)+0(t^2) \end{aligned}\right\} \tag{132}$$

where σ_2 and τ_2 are 0(1). Then, by (89) and (90)

$$\eta=1-\tfrac{1}{2}(\tau_2^2-\sigma_2^2)t^2+\ldots\ , \qquad \zeta=\sigma_2\tau_2t^2+\ldots \tag{133}$$

$$\frac{\gamma'}{\gamma}=\frac{\sigma_2}{\sigma_2^2+\tau_2^2}\left(\frac{\sigma_2^2+\tau_2^2}{\sigma_2}\right)'+\ldots\ . \tag{134}$$

with these expressions equations (93) become

$$F=\frac{\tau_2(\tau_2^2-\sigma_2^2)}{4\sigma_2^2(\sigma_2^2+\tau_2^2)t}+\dots \quad , \qquad G=\frac{\sigma_2}{2(\sigma_2^2+\tau_2^2)t}+\dots \quad . \tag{135}$$

All the terms in (131) are now of the same order. Equating the leading terms gives

$$-s(\tau_2^2-\sigma_2^2)'=\frac{2\tau_2(\tau_2^2-\sigma_2^2)}{\sigma_2^2(\sigma_2^2+\tau_2^2)}+\frac{s(\tau_2^2-\sigma_2^2)\sigma_2}{\sigma_2^2+\tau_2^2}\left(\frac{\sigma_2^2+\tau_2^2}{\sigma_2}\right)' \tag{136}$$

and

$$s(\sigma_2\tau_2)'=\frac{2\sigma_2}{\sigma_2^2+\tau_2^2}-\frac{s\sigma_2^2\tau_2}{\sigma_2^2+\tau_2^2}\left(\frac{\sigma_2^2+\tau_2^2}{\sigma_2}\right)' \quad , \tag{137}$$

where primes denote differentiation with respect to x and s is now constant.

Equation (137) can be rearranged as

$$(\tau_2(\sigma_2^2+\tau_2^2))'=2/s \quad ,$$

which can be integrated downstream from $x=x_0$. At $x=x_0$, $\xi=0$ and the upstream solution is given by equation (109):

$$\sigma=\sigma_1(0)t^n+\dots \quad , \qquad \tau=\tau_1(0)t+\dots \quad ,$$

where $\sigma_1^2(0)=4\Gamma(1/l)/s\tau_1 l\lambda^{2/l}$ by equation (120),

$\tau_1(0)=\tau_1=(4/A(x_0))^{1/3}$ by equation (116),

and λ and l are related to the local shape of the planform through equations (112) and (118). Hence

$$\tau_2(\sigma_2^2+\tau_2^2)=2(x-x_0+k)/s \tag{138}$$

where, with equations (117),

$$k=\frac{2s}{A(x_0)}+\frac{2}{l}\Gamma\left(\frac{1}{l}\right)\left(\frac{t}{\lambda}\right)^{2/l} \quad . \tag{139}$$

Knowing the integral (138), we can proceed to solve equation (136) to obtain σ_2 and τ_2 separately. One way is to write $\sigma_2^2=\mu\tau_2^2$ in equations (136) and (138), which eventually leads to the equation

$$\frac{\mu'}{1-\mu}=\frac{2}{x-x_0+k} \quad .$$

The solution of this is immediate: $\mu=1-K/\chi^2$, where

$$\chi=x-x_0+k \quad , \tag{140}$$

and K is given by the initial condition at $x=x_0$, $\chi=k$, as

$$K=k^2\left(1-\frac{A(x_0)}{sl}\Gamma\left(\frac{1}{l}\right)\left(\frac{t}{\lambda}\right)^{2/l}\right) \quad . \tag{141}$$

With this expression for μ, equation (138) gives

and

$$\left.\begin{aligned}\sigma_2&=(\chi^2-K)^{1/2}/[s(\chi^2-\tfrac{1}{2}K)]^{1/3}\\ \tau_2&=\chi/[s(\chi^2-\tfrac{1}{2}K)]^{1/3} \quad .\end{aligned}\right\} \tag{142}$$

Equations (132) and (139) to (142) give the formal solution required.

It is interesting to note how k and K depend partly on the overall shape of the wing ahead of $x = x_0$ through s and $A(x_0)$, and partly on the local shape near $x = x_0$ through λ and l. The structure of the solution depends on the value of l. We avoid discussion of the general case by considering the ordinary streamwise tip, which has a continuous tangent and a curvature which is discontinuous, but finite. This is given by $l = 2$.

With $l = 2$, equations (142) become

$$\sigma_2 = A_0^{1/6}(A_0\bar{\xi}^2 + 4\bar{\xi} + 2\sqrt{\pi t}/\lambda s)^{1/2}/(A_0^2\bar{\xi}^2 + 4A_0\bar{\xi} + 2)^{1/3}$$

and

$$\tau_2 = (A_0\bar{\xi} + 2)/A_0^{1/3}(A_0^2\bar{\xi}^2 + 4A_0\bar{\xi} + 2)^{1/3}$$

where $\bar{\xi} = (x - x_0)/s$ is a non-dimensional coordinate measured downstream on the parallel-sided part of the wing and $A_0 = A(x_0)$ is the aspect ratio of the upstream part. The coordinates of the vortex in the cross-flow plane follow from equation (133), its strength from equation (90) and the lift acting upstream of the plane $x = \text{const}$ from equation (94):

$$\left.\begin{aligned} \eta &= 1 - \frac{2t^2}{[A_0(A_0^2\bar{\xi}^2 + 4A_0\bar{\xi} + 2)]^{2/3}} + 0(t^3) \quad , \\ \zeta &= \frac{(A_0\bar{\xi} + 2)(A_0\bar{\xi}^2 + 4\bar{\xi} + 2\sqrt{\pi t}/\lambda s)^{1/2} t^2}{A_0^{1/6}(A_0^2\bar{\xi}^2 + 4A_0\bar{\xi} + 2)^{2/3}} + 0(t^3) \quad , \\ \Gamma &= \gamma Us = \frac{8\pi Us(A_0^2\bar{\xi}^2 + 4A_0\bar{\xi} + 2)^{2/3} t^4}{A_0^{5/6}(A_0\bar{\xi}^2 + 4\bar{\xi} + 2\sqrt{\pi t}/\lambda s)^{1/2}} + \ldots \end{aligned}\right\} \tag{143}$$

and

$$L = \pi\rho U^2 s^2 \alpha(1 + 4(A_0^2\bar{\xi}^2 + 4A_0\bar{\xi} + 2)^{1/3} t^2/A_0^{2/3} + \ldots) \quad .$$

These expressions can be compared with the much simpler upstream solutions (104) to (107). The orders of the leading terms in the expansions of ζ and Γ change: ζ is of order t^3 for $x < x_0$, order t^2 for $x > x_0$ and order $t^{5/2}$ for $x = x_0$; Γ is also of order t^3 for $x < x_0$, but becomes order t^4 for $x > x_0$ and order $t^{7/2}$ for $x = x_0$. The terms in the expansions of η and L remain of the same order, but their coefficients become more complicated for $x > x_0$. Some simplification is gained by introducing the local aspect ratio, $A(x) = 2A_0/(A_0\bar{\xi} + 2)$, in, for instance, the last equation:

$$C_L = L/\tfrac{1}{2}\rho U^2 S(x) = \frac{\pi}{2}A(x)\alpha\left(1 + 2\left(2 - \frac{A^2(x)}{A_0^2}\right)^{1/3}\left(\frac{\alpha}{A(x)}\right)^{2/3} + \ldots\right) \quad , \tag{144}$$

for $x \geqslant x_0$. The change to the parallel-sided part of the wing has introduced the factor $(2 - A^2(x)/A_0^2)^{1/3}$ on the non-linear term in the lift. As x increases, $A(x)$ falls from A_0 to zero and the coefficient increases slightly. It is of some interest that the non-linear part of the lift coefficient, as given by equations (144) or (107), falls to zero as the aspect ratio tends to zero, though more slowly than the linear part. It is not clear how the inclusion of higher order terms would affect this result.

Finally it is worth noting the simple forms assumed by equations (143) for stations well downstream on the parallel-sided part of the wing:

$$\left.\begin{aligned} \eta &\sim 1 - \frac{2}{A_0^2}\bar{\xi}^{-4/3}\left(\frac{\alpha}{4}\right)^{2/3} \sim 1 - \frac{A^2}{2A_0^2}\left(\frac{\alpha}{2A}\right)^{2/3} \quad , \\ \zeta &\sim \bar{\xi}^{2/3}(\alpha/4)^{2/3} \sim (\alpha/2A)^{2/3} \quad , \\ \Gamma &\sim 8\pi Us\bar{\xi}^{1/3}(\alpha/4)^{4/3} \sim 2\pi\alpha Us(\alpha/2A)^{1/3} \end{aligned}\right\} \tag{145}$$

and

$$L \sim \pi\rho U^2 s^2 \alpha(1 + 4(\alpha/2A)^{2/3}) \quad ,$$

where the approximation is for α small, $\bar{\xi}$ large and A small. It is only in the first of these expressions that any trace of that part of the wing upstream of $x = x_0$ remains, and there it only affects the rate at which the vortices move to positions above the side edges far downstream. The vortex height, its strength and the lift are (to this order) independent of the upstream part of the wing. It is therefore plausible to regard the last three of equations (145) as applying generally, even to cropped delta or rectangular wings, for which they could not have been derived by the present arguments.

4.5 Comparison with Numerical Solutions

It is not in general possible to assess the range of validity of asymptotic expansions, such as those derived in this Report, except by comparison with complete solutions. For the present problem, a complete solution must be numerical. Fortunately numerical solutions can easily be computed and several years ago the method described in Ref. 11 was programmed and solutions were found for several planforms over a range of angles of incidence. For the present purpose the results obtained for a gothic wing provide a convenient comparison.

We consider first the overall lift and the centre of pressure. A convenient and sensitive way of displaying the non-linear variation in lift with incidence is to plot $C_L/\alpha A$ against α/A, since this function depends only on α/A and is constant for attached flow. Its asymptotic expansion follows at once from equation (107):

$$\frac{C_L}{\alpha A} = \frac{\pi}{2}\left(1 + 2\left(\frac{\alpha}{A}\right)^{2/3} + \ldots\right) \quad . \tag{146}$$

The distance, h, of the centre of pressure from the apex is given by

$$hL(1) = \int_0^1 x\frac{dL}{dx}dx = L(1) - \int_0^1 L(x)dx \quad ,$$

for a wing of unit length, and $L(x)$ is given by equation (124) for a gothic wing. The linear term in $L(x)$ is easily integrated analytically. The non-linear term was integrated numerically by Simpson's rule over 10 intervals, leading to:

$$h = \frac{7}{15}\left(1 + 0{\cdot}50\left(\frac{\alpha}{A}\right)^{2/3} + \ldots\right) \quad . \tag{147}$$

Fig. 7 displays the approximations (146) and (147) as curves, compared with the points obtained by numerical integration of the basic equations (91) and (92). The single-term asymptotic expansion reflects the qualitative behaviour of both the lift and the centre of pressure over this range of values of α/A quite satisfactorily. In quantitative terms, the error is about 20 per cent in non-linear lift (7 per cent of overall lift) at $\alpha/A = 0{\cdot}1$, which seems intuitively to be rather large. It appears less surprising if it is recalled that the expansion parameter is $(\alpha/A)^{1/3}$, which is about $0{\cdot}5$ when $\alpha/A = 0{\cdot}1$.

Fig. 7 suggests that the range of validity of the single-term asymptotic expansion is rather small, so the smallest value of α/A ($0{\cdot}0279$) used in the numerical calculations was chosen for a closer examination of the results. The lateral position of the vortex is given by equations (124). For its height above the wing, we have three different asymptotic expansions: the outer (124), valid away from the trailing edge; the inner (127), valid near the trailing edge; and the composite (129), valid over the whole length of the wing. Fig. 8 shows how these expansions compare with the numerical solutions for $\alpha/A = 0{\cdot}0279$. It is clear that the single-term asymptotic expansion for the lateral position of the vortex is not a reliable approximation at this value of α/A. Near the apex, where the wing approximates to a delta wing of $\alpha/A = 0{\cdot}0105$, the asymptotic expansion is good, and the deterioration as x increases is associated with an increase in local sweepback of the leading edge. For delta wings, the accuracy of the single-term expansion also deteriorates in an obvious way as the sweepback increases and the incidence is constant. The variation in the height of the vortex along the length of the wing is well described by the single-term composite expansion, though again the error increases as the local sweepback increases. The outer expansion diverges as the trailing edge is approached, so the improvement brought about by the use of the inner expansion is striking. It is remarkable that the composite expansion is closer to the numerical results than either the inner or the outer expansion over the whole length.

The circulation of the vortex is also described by an outer expansion (124), an inner expansion (128) and a composite expansion (130). These are compared with the numerical calculation for the same test case in the upper part of Fig. 9. All show a decrease in circulation towards the rear of the wing, as reported in Ref. 11,

which must be associated with the shedding from the leading edge of vorticity of the opposite sense. The composite expansion is quite successful in describing the variation of the circulation.

The distribution of non-linear lift is shown in the lower part of Fig. 9 in terms of the ratio of the total lift acting forward of the station x = constant to the linear, attached flow, prediction of the lift forward of the same station. From equations (123) and (124)

$$L_{\text{lin}} = \pi\rho U^2 \alpha s^2(x) = \pi\rho U^2 \alpha A^2 x^2 (2-x)^2/9 \quad ,$$

and the single-term asymptotic expansion is given by

$$\frac{L}{L_{\text{lin}}} = 1 + 2\left(\frac{\alpha}{A}\frac{3-x}{2(2-x)^2}\right)^{2/3} \quad .$$

This expansion correctly predicts that the non-linear lift becomes a greater part of the total as the sweep increases rearwards. The non-linear lift is slightly underestimated near the apex, and increasingly so further aft. This explains the discrepancies in lift and centre of pressure apparent in Fig. 7 at this value of α/A.

4.6 An Application of the Asymptotic Solution

In view of the relative ease with which the numerical solution can be calculated and the limited range of applicability of the asymptotic expansion, the utility of the latter is obviously limited. However, it does perform the minimum role of an analytic treatment in suggesting a useful way to look at experimental results.

Almost all calculations of aerodynamic properties are based on the assumption that the flow remains attached, while experiments with plane, sharp-edged, slender wings show that the flow separates from the leading edges at very small angles of incidence. Theoretical models of the separated flow agree that the lift-curve slope, $\partial C_L/\partial\alpha$, and the aerodynamic centre, $\partial C_m/\partial C_L$, are given by their attached-flow values when the angle of incidence of the plane wing is zero. In order to assess the accuracy of the calculations for attached flow it is necessary to derive the lift slope and aerodynamic centre at zero incidence from measurements. The usual method is to plot C_L/α and C_m/C_L against α or C_L and extrapolate to find the ordinate at zero lift and incidence. The limitations on the accuracy of measurement make this procedure difficult and the difficulty is increased by ignorance of the form of the dependence of these quantities on the incidence.

An example, taken from Kirby[17], is shown on the left of Fig. 10, where the normal force coefficient C_N has been used in place of C_L. The measurements were made on the overhead balance of the 4ft × 3ft tunnel at Farnborough at 200 fps, Reynolds number 2·2 million, with free transition. The model was a sharp-edged delta wing of aspect ratio one, with a maximum thickness-chord ratio of 4 per cent. The scatter in the derived values of C_N/α at small angles of incidence is not unusually large, this example being chosen because the large number of measured values makes it clear that limitations on accuracy rather than systematic error are responsible. The curve is that given in Ref. 17 as a best fit to the measurements and it appears to be a good one. On the right of the figure, the same values of C_N/α are plotted against $|\alpha|^{2/3}$, and a straight line is drawn by eye through the points, discounting those which are most scattered.

Two facts stand out: the use of $\alpha^{2/3}$ has produced a more linear relation, as would be expected from equation (107), and the extrapolated value of C_N/α at $\alpha = 0$ is about 10 per cent lower on the right than on the left. Since the apparently linear part of the curve extends to values of α larger than those for which the present treatment is reliable, there is an element of good fortune about the straight-line fit. The important point is that the form of the asymptotic solution provides the justification for the linear extrapolation in the region where the experimental values are no longer a reliable guide. The significance of a 10 per cent difference in the value of the lift-curve slope at zero lift, as derived from measured values, becomes apparent when we recall that it is this quantity which we should compare with an estimate for attached flow (based on lifting-surface theory, for instance), in order to determine the importance of boundary layer and wake effects in the absence of leading-edge separation. For two-dimensional aerofoils at low speeds the reduction in lift due to these effects is normally less than 10 per cent.

5. Wings with Lengthwise Camber

This section examines a second non-conical flow in which we take the edges of the wing to be straight lines but we allow the local angle of incidence of the wing to vary along its length. The wings considered are specified

by their local semi-span and incidence by the equations

$$s(x) = A_0 + A_1 x$$

and

$$\alpha(x) = K_1 x^n \tag{148}$$

where A_0 is a non-negative constant, and K_1 and n are positive constants. The wings take the general form of the truncated delta wing shown in Fig. 11, with the unswept part of the leading edge at zero local incidence. Delta wings are obtained with $A_0 = 0$, $A_1 > 0$; while with $A_0 > 0$, a wing with an unswept leading edge, and raked-in, streamwise, or raked-out tips is obtained, as A_1 is negative, zero, or positive.

The method used here is based on that used by Smith[11] in his application of the line-vortex model to wings with curved leading edges. No separation takes place from the unswept part of the leading edge; it is assumed that separation takes place at the other edges of the planform and this separation is modelled in the same way whether the edge is leading or trailing in a geometrical sense. The Kutta condition is imposed at the edge, and the zero force condition is imposed on the vortex and cut, leading to ordinary differential equations for the vortex position and strength as functions of the downstream distance x. Since we are interested in the initial growth of the vortices close to the station of zero incidence we shall find asymptotic solutions to these equations valid for small x.

5.1 Derivation of Vortex Equations

The configuration is shown in Fig. 11 with the rectangular axes $0xyz$ fixed with respect to the wing with $0x$ parallel to the free stream. In the cross-flow plane, x = constant, we introduce a set of parallel axes $0'y'z'$ in which the origin is on the wing centre line, and a complex coordinate Z defined by

$$Z = y' + iz' = y + i(z + h) \tag{149}$$

where $h(x)$ is the distance of the wing centre line below the x-axis, so that $h'(x) = \alpha(x)$ is the local incidence.

The flow in the cross-flow plane can now be represented by a velocity potential

$$\Phi - Uz'h'(x)$$

where the boundary conditions require that $\partial\Phi/\partial z'$ should be equal to $Uh'(x)$ for large z' and be zero on the wing. Under the slender-body assumptions the velocity potential Φ must satisfy Laplace's equation in the cross-flow plane, and so it can be written as the real part of an analytic function W, the complex velocity potential.

As in Ref. 11 we make use of the conformal transformation

$$Z^{*2} = Z^2 - s^2 \tag{150}$$

which maps the wing into a slit on the imaginary axis, the plane of symmetry in the Z^*-plane. The complex velocity potential becomes

$$W = -i\alpha U Z^* + \frac{\Gamma}{2\pi i} \ln \frac{Z^* - Z_v^*}{Z^* + \bar{Z}_v^*} \quad , \tag{151}$$

where the vortex strength Γ and its position in the transformed plane Z_v^* are to be determined from further conditions on the vortex system. These conditions are provided by the Kutta condition, requiring that the edge should be a stagnation point in the Z^*-plane, and the zero force condition, which requires that the total force on each vortex and its cut should vanish.

Introducing the non-dimensional quantities

$$Z_1^* = Z_v^*/s$$

$$Z_1 = Z_v/s$$

and

$$\gamma = \Gamma/(2\pi U s) \quad , \tag{152}$$

the Kutta condition becomes

$$\gamma = \frac{\alpha Z_1^* \bar{Z}_1^*}{Z_1^* + \bar{Z}_1^*} \quad . \tag{153}$$

The force per unit length acting on the cut has been derived by Smith[11] and is

$$i\rho U(Z_v - s)\frac{d\Gamma}{dx} \quad , \tag{154}$$

and the zero force condition requires this to be balanced by the force exerted on the corresponding line vortex. This contribution will be given by the product of $-i\rho\Gamma$ and the component of velocity normal to the vortex induced by the remainder of the flow. The axial velocity U will contribute a component

$$-U\frac{d}{dx}(y_v + iz_v) = -U\frac{d}{dx}(Z_v - ih) \tag{155}$$

normal to the vortex, whilst the normal component of the cross-flow velocity is

$$\lim_{Z \to Z_v} \overline{\left(\frac{dW}{dZ} - \frac{\Gamma}{2\pi i}\frac{1}{Z - Z_v}\right)} - ih'(x)U \quad . \tag{156}$$

Using equations (150), (151) and (153) the complex conjugate of this limit can be expressed as

$$\frac{\Gamma}{2\pi i}\frac{Z_v}{Z_v^*}\left(\frac{Z_v^* + \bar{Z}_v^*}{Z_v^*\bar{Z}_v^*} - \frac{1}{Z_v^* + \bar{Z}_v^*} - \frac{s^2}{2Z_v^2\bar{Z}_v^*}\right) \quad ,$$

and this can be combined with (154) and (155) to give the zero force condition in the form

$$(\bar{Z}_1 - 1)\frac{d}{dx}(\gamma s) + \gamma\frac{d}{dx}(\bar{Z}_1 s) = \frac{\gamma^2}{i}\frac{Z_1}{Z_1^*}\left(\frac{Z_1^* + \bar{Z}_1^*}{Z_1^*\bar{Z}_1^*} - \frac{1}{Z_1^* + \bar{Z}_1^*} - \frac{1}{2Z_1^2 Z_1^*}\right) \quad , \tag{157}$$

where we have used the non-dimensional quantities defined by equation (152). This expression agrees with that given in equation (8) of Ref. 11 for a flat-plate wing.

Using equations (148) and (153) we can rearrange this equation to give

$$(A_0 + A_1 x)\frac{d}{dx}\left(\frac{(\bar{Z}_1 - 1)Z_1^*\bar{Z}_1^* x^n}{Z_1^* + \bar{Z}_1^*}\right) + A_1\frac{(2\bar{Z}_1 - 1)Z_1^*\bar{Z}_1^* x^n}{Z_1^* + \bar{Z}_1^*}$$

$$= \frac{K_1 x^{2n}}{i}\frac{Z_1^{*2}\bar{Z}_1^{*2}}{(Z_1^* + \bar{Z}_1^*)^2}\frac{Z_1}{Z_1^*}\left(\frac{Z_1^* + \bar{Z}_1^*}{Z_1^*\bar{Z}_1^*} - \frac{1}{Z_1^* + \bar{Z}_1^*} - \frac{1}{2Z_1^2 Z_1^*}\right) \quad . \tag{158}$$

We now introduce the real and imaginary parts of Z_1 and Z_1^* by

$$Z_1 = 1 - \lambda + i\mu$$

and

$$Z_1^* = \sigma + i\tau \quad , \tag{159}$$

so that from the conformal transformation (150)

$$\sigma^2 - \tau^2 = \lambda^2 - 2\lambda - \mu^2 \tag{160a}$$

and

$$\sigma\tau = (1 - \lambda)\mu \quad . \tag{160b}$$

Substituting equations (159) and (160b) into equation (158) and equating real and imaginary parts leads to

$$(A_0+A_1x)\frac{d}{dx}\left(\frac{\lambda}{\sigma}(\sigma^2+\tau^2)x^n\right)-A_1\frac{(1-2\lambda)(\sigma^2+\tau^2)}{\sigma}x^n$$
$$=\frac{K_1x^{2n}}{4\sigma^2\mu}\left((\tau^2-\mu^2)(3\sigma^2-\tau^2)-\frac{2\sigma^2\tau^2+\mu^2(\sigma^2-\tau^2)}{(1-\lambda)^2+\mu^2}\right) \quad , \tag{161a}$$

and

$$(A_0+A_1x)\frac{d}{dx}\left(\frac{\mu}{\sigma}(\sigma^2+\tau^2)x^n\right)+A_1\frac{2\mu(\sigma^2+\tau^2)}{\sigma}x^n$$
$$=\frac{K_1x^{2n}}{4\sigma^2\mu}\left(\frac{\tau(\sigma^2+\mu^2)(3\sigma^2-\tau^2)}{\sigma}-\frac{\sigma\tau(\sigma^2-\tau^2-2\mu^2)}{(1-\lambda)^2+\mu^2}\right) \quad . \tag{161b}$$

We can now proceed to find asymptotic solutions to equations (160) and (161). Four separate cases arise corresponding to different choices for the planform parameters A_0 and A_1. Thus for $A_1=0$ and $A_0>0$ the planform will be rectangular, for $A_0=0$ and $A_1>0$ it will be be delta shaped, for A_0 and A_1 both positive the planform will be that of a truncated delta wing or an unswept wing with a raked-out tip, and for $A_0>0$ and $A_1<0$ it will be an unswept wing with a raked-in tip.

5.2 The Rectangular Wing

It emerges that a solution can be found only if σ and τ are of the same order of magnitude, so that to first order we can write

$$\sigma=Ax^p \quad , \qquad \tau=k\sigma \tag{162}$$

where A, k and p are constants. Again retaining only the first order terms, substitution in equation (160) yields

$$\mu=kA^2x^{2p} \quad , \qquad \lambda=-\tfrac{1}{2}A^2(1-k^2)x^{2p} \quad . \tag{163}$$

These equations can now be substituted into equation (161) with $A_1=0$ and the resulting expressions simplified retaining only the leading terms in x to give

$$-\tfrac{1}{2}(3p+n)A^3(1-k^4)x^{3p+n-1}=\frac{1}{4s}K_1k(1-k^2)x^{2n} \tag{164}$$

and

$$(3p+n)A^3k(1+k^2)x^{3p+n-1}=\frac{K_1}{2s}x^{2n} \quad . \tag{165}$$

Comparison of these two equations indicates that we must have $k^2=1$, and since σ, and hence A, must be positive we can see from equation (165) that k must be positive, so that $k=1$. Since each side of equation (165) must be of the same order in x it follows that

$$p=\frac{1}{3}(n+1) \quad , \tag{166}$$

and from equation (165)

$$A=\left(\frac{K_1}{4A_0(2n+1)}\right)^{1/3} \quad . \tag{167}$$

In terms of these two constants the vortex position is given by

$$Z_v^* = As(1+i)x^p + \ldots \tag{168}$$

in the transformed plane and by

$$Z_v = s(1+iA^2x^{2p}) + \ldots \tag{169}$$

in the physical cross-flow plane.

The application of slender-body theory to the rectangular wing is only justifiable if the local incidence vanishes at the leading edge, i.e. if $n > 0$. However, it is interesting to consider the limit $n \to 0$, in which the incidence tends to the constant value k_1. We have $p \to 1/3$, so that the vortex position (169) becomes

$$Z_v = s\left(1+i\left(\frac{\alpha x}{4s}\right)^{2/3}\right) \quad .$$

This is the same behaviour as that described by equation (145) for the vortex position on the parallel-sided part of a wing at a small, constant angle of incidence α, well downstream of the station at which the span became constant. Approaching the rectangular wing at uniform incidence from two quite different directions thus leads to the same result.

5.3 The Delta Wing

If we choose A_0 to be zero and A_1 to be positive then the planform reduces to that of a delta wing. It is found that choosing σ and τ to be of the same order of magnitude no longer leads to a consistent first-order solution to the equations and so we now look for a solution of the form

$$\sigma = Ax^p \quad , \qquad \tau = Bx^q \tag{170}$$

where A, B, p and q are constants, and where we make the further assumption, based on the results for plane delta wings, that $p > q$.

From equations (160) we find that, to first order

$$\mu = ABx^{p+q} \quad , \qquad \lambda = \tfrac{1}{2}B^2x^{2q} \quad , \tag{171}$$

and when these expressions are substituted into equations (161) we obtain to first order

$$\frac{A_1B^2}{A}x^{n+2q-p} = \frac{K_1B^3}{4A^3}x^{2n+3q-3p} \tag{172a}$$

and

$$(n+3q+2)A_1B^3x^{n+3q} = \tfrac{1}{2}K_1x^{2n} \quad . \tag{172b}$$

These two equations can now be solved to give

$$q = n/3 \quad , \qquad B = \left(\frac{K_1}{4A_1(n+1)}\right)^{1/3} \tag{173a}$$

and

$$p = 2n/3 \quad , \qquad A = \left(\frac{K_1B}{4A_1}\right)^{1/2} \quad . \tag{173b}$$

The vortex position in the transformed plane is given by

$$Z_v^* = s(Ax^{2n/3} + iBx^{n/3}) + \ldots \tag{174a}$$

and in the physical plane by

$$Z_v = s(1 - \tfrac{1}{2}B^2 x^{2n/3} + iABx^n) \quad . \tag{174b}$$

It should be noted that for $n = 0$ the wing becomes a plane delta wing over which the flow will be conical. The solution given by equation (173) now becomes

$$Z_v^* = s(B^2 + iB) \tag{175}$$

where $B = (K_1/4A_1)^{1/3}$, and this agrees with the leading term in the expansion given in Ref. 1.

The height of the vortex above the wing takes a simple form. For this non-dimensional height we have, from equations (174), (148) and (173),

$$\mathcal{I}\{Z_v/s\} = \alpha(x)/(4A_1(n+1)^{1/2}) \quad . \tag{176}$$

Expressed as a fraction of the distance of the wing below the x-axis, the vortex height becomes

$$\mathcal{I}\{Z_v/h\} = \tfrac{1}{4}(n+1)^{1/2} \quad , \tag{177}$$

and these two equations represent simple generalisations of the corresponding results for the plane wing, for which $n = 0$.

5.4 The Truncated Delta Wing or Raked-Out Tip

If we assume that both A_0 and A_1 are positive, then the resulting planform is that of the truncated delta wing. As in the previous case we look for a solution for which $\sigma \ll \tau$, so that we can assume that the leading terms in the expansion for the vortex position are still given by equations (170) and (171) with $p > q$. Substituting these expressions into equation (161b) and retaining the leading terms on either side, we obtain

$$A_0 \frac{d}{dx}(B^3 x^{n+3q}) = \tfrac{1}{2}K_1 x^{2n} \tag{178}$$

from which it follows that

$$q = (n+1)/3 \quad , \qquad B = \left(\frac{K_1}{2(2n+1)A_0}\right)^{1/3} \quad . \tag{179}$$

Similarly from equation (161a)

$$A_0 \frac{d}{dx}\left(\frac{B^4}{2A} x^{n+4q-p}\right) - \frac{A_1 B^2}{A} x^{n+2q-p} = -\frac{K_1 B^3}{4A^3} x^{2n+3q-3p} \quad , \tag{180}$$

and using the value for q given by equation (179) we can see that the second term in the left-hand side of equation (180) will dominate provided that $n > \frac{1}{2}$. In this case the first term can be neglected and so

$$p = \frac{1}{6}(4n+1) \quad , \qquad A = \left(\frac{K_1 B}{4A_1}\right)^{1/2} \quad , \tag{181}$$

and the vortex position will be given in terms of these constants. If, however, $n < \frac{1}{2}$ then the first term in equation (180) dominates, and since $(n+4q-p)$ and B will both be positive there can be no solution to equation (180). The reason is that, as can be seen from equations (179) and (181), the original assumption that $p > q$ will no longer hold if $n \leq \frac{1}{2}$.

Therefore, for the case $0 < n < \frac{1}{2}$, we look for a solution in which σ and τ are the same order of magnitude so that we can assume that equations (162) and (163) hold. The leading term in the solution will in fact be the same as that obtained for the rectangular wing in equations (166) and (167) since it can easily be checked that the terms involving A_1 in the left-hand sides of equations (161) will be small compared to those terms retained in equations (164) and (165). The vortex position for this case will therefore be the same as that given by equations (168) and (169).

When $n = \frac{1}{2}$ a different dependence emerges, details of which are given in Table 1.

The original problem, derived from an attempt to describe the flow over a wing with lengthwise camber, is the one for which, at $x = 0$, the local incidence has a simple zero, i.e. $n = 1$, the span is non-zero, i.e. $A_0 \neq 0$, and the span is increasing, i.e. $A_1 > 0$. For this case we have $p = 5/6$ and $q = 2/3$ from (179) and (181). Using the relations set out above, we find the vortex position, Z_v, in the cross-flow plane is given by

$$\frac{Z_v}{s} = 1 - \frac{1}{2}\left(\frac{\alpha}{s'}\right)^{2/3}\left(\frac{s'x}{6s}\right)^{2/3} + \frac{i}{2}\frac{\alpha}{s'}\left(\frac{s'x}{6s}\right)^{1/2} + \ldots \quad , \tag{182}$$

where A_0, A_1 and K_1 have been replaced by s, s' and α/x respectively, and the circulation, Γ, is given by

$$\frac{\Gamma}{Us} = 2\pi\alpha\left(\frac{s'x}{6s}\right)^{1/2} + \ldots \quad . \tag{183}$$

This behaviour appears physically plausible, remembering that α is proportional to x, except for the behaviour of the height and strength of the vortex for small values of s'. If s' is actually zero, the rectangular wing solution of Sub-section 5.2 applies and the vortex height becomes of order $x^{4/3}$ instead of $x^{3/2}$, while the circulation becomes of order $x^{5/3}$ instead of $x^{3/2}$. If a uniformly valid expansion for s' small is required a matching process like that in Section 4.3 should be used.

It is hoped that the asymptotic forms (182) and (183) will be helpful in modelling the initial growth of the second vortex which is shed from the rearward part of the leading edge of a wing with lengthwise camber. At least they make it clear that a conical growth is not to be expected.

5.5 The Raked-In Tip

If we assume that A_0 is positive and A_1 negative, we obtain a planform with an unswept leading edge and a raked-in tip. Geometrically, the tip is now a trailing edge. The unswept leading edge is at zero local incidence and so the same flow model, using slender-body theory and representing separation from the swept edge only, is still appropriate.

There are now no asymptotic solutions to equations (160) and (161) with $\sigma \ll \tau$, essentially because the sign of the second term on the left-hand side of equation (180) has changed and the term cannot balance the right-hand side. With $\sigma \gg \tau$, i.e. $p < q$, introducing (170) and (171) into (161b) and discarding higher-order terms leads to:

$$A_0\frac{d}{dx}(A^2 B x^{n+2p+q}) = \tfrac{1}{2}K_1 x^{2n} \quad , \tag{184}$$

in place of equation (178). The same procedure applied to equation (161a) leads to:

$$-A_0\frac{d}{dx}(\tfrac{1}{2}A^3 x^{n+3p}) - A_1 A x^{n+p} = \frac{K_1 B}{4A}x^{2n+q-p} \quad , \tag{185}$$

in place of equation (180). Equating indices in equation (184) shows that $2n+q-p = n+p+2q-1$, which exceeds $n+3p-1$, by the assumption that $q > p$. Hence the right-hand side of equation (185) is of higher order than the terms on the left. Equating the left-hand side to zero gives:

$$p = \tfrac{1}{2} \quad , \qquad A = \left(-\frac{4A_1}{(2n+3)A_0}\right)^{1/2} \quad . \tag{186}$$

Introducing equation (186) into equation (184) now gives:

$$q = n \quad , \qquad B = -\frac{(2n+3)K_1}{8(2n+1)A_1} \quad . \tag{187}$$

Since we have assumed that $q > p$, this solution is only valid for $n > \frac{1}{2}$.

To find solutions for $n \leqslant \frac{1}{2}$, we suppose $p = q$ and use the formulation of (162) and (163). Introducing this into equation (161b) and discarding the higher-order terms leads to:

$$A_0 \frac{d}{dx}(k(1+k^2)A^3 x^{n+3p}) = \tfrac{1}{2}K_1 x^{2n} \quad , \tag{188}$$

from which

$$p = \frac{n+1}{3} \quad , \qquad A = \left(\frac{K_1}{2k(1+k^2)(2n+1)A_0}\right)^{1/3} \quad . \tag{189}$$

The same process applied to equation (161a) leads to:

$$A_0 \frac{d}{dx}\left(-\frac{A^3}{2}(1-k^4)x^{n+3p}\right) - A_1 A(1+k^2)x^{n+p} = \frac{K_1 k(1-k^2)x^{2n}}{4} \quad . \tag{190}$$

The first term is now of the same order as the right-hand side, by equation (189), so there are two possibilities: either these two terms are equal and dominate the second term on the left, or all three terms are of the same order. If they dominate the second term, $p > n$, $n < \frac{1}{2}$ and

$$-\tfrac{1}{2}A_0 A^3(1-k^4)(2n+1) = \tfrac{1}{4}K_1 k(1-k^2) \quad .$$

This is only compatible with equation (189) if $k^2 = 1$, implying $\sigma = \tau$, since both are positive. Hence, for $n < \frac{1}{2}$, we have

$$p = q = \frac{n+1}{3} \quad , \qquad A = B = \left(\frac{K_1}{4(2n+1)A_0}\right)^{1/3} \quad . \tag{191}$$

If, on the other hand, all the terms in equation (190) are of the same order, introducing expressions (189) into equation (190) shows that $n = p = \frac{1}{2}$ and the coefficients A and B satisfy quartic equations.

The essential features of the results obtained in Section 5 are summarised in tabular form in Table 1. Here, B_0 is a root of the quartic equation:

$$4A_1 B(4A_0 B^3 - K_1) + K_1(8A_0 B^3 - K_1) = 0 \quad . \tag{192}$$

For $A_1 > 0$, this equation has a single positive real root, which must therefore be chosen. For $A_1 < 0$, the equation has two positive real roots, of which the smaller must be chosen to ensure that A is also real.

It is noteworthy that for $0 < n < \frac{1}{2}$, the effect of the rapid increase in the angle of incidence dominates the effect of the change in local span, so that the solutions tabulated are independent of A_1. The same solution is naturally found for all values of $n > 0$ for the rectangular wing. In this solution σ and τ are the same, so the vortex lies directly above the leading edge, in this first approximation. For $n \geqslant \frac{1}{2}$, which includes the most interesting case ($n = 1$) of a regular variation of the angle of incidence, the effect of the variation in span becomes important and the solutions differ in the leading term. For the raked-out tip, or truncated delta wing, $\tau \gg \sigma$ and the vortex lies inboard of the edge of the planform. For the streamwise tip the vortex lies above the leading edge, and for the raked-in tip, $\sigma \gg \tau$ and the vortex lies outboard of the planform edge.

Acknowledgments

The authors thank N. Riley of the University of East Anglia for pointing out the need for matched expansions in the problem of Section 4, E. C. Maskell for providing details of his similarity relations and S. P. Fiddes for providing the solution given in Sub-section 5.5.

LIST OF SYMBOLS

$a =$	α/K incidence parameter
a_0	Attachment incidence parameter for half-circular cone
a_0, a_1, a_2	*See* equation (B-4)
$A(x)$	Local aspect ratio
A_0, A_1	*See* equation (148)
A, B	*See* equations (162) and (170) or (112)
b_0, b_1, b_2	*See* equation (B-4)
B_0, B_1	Functions of ε, *see* equation (9)
c	*See* equation (B-2), also used as wing chord in Section 4
C_L	Lift coefficient
d	Semi-span of rhombic wing in transformed plane
F, G	*See* equation (93) or (A-1) and (A-2)
$f(n, P), g(n, P)$	*See* equations (67) and (68)
$g(\bar{\xi})$	*See* equation (126)
$h(x)$	Camber of wing centre line
k	Constants, *see* equations (13), (139) or (162)
$K =$	s/x. *See also* equation (141)
K_1	*See* equation (148)
l	*See* equation (112)
$L(x)$	Lift acting on wing upstream of the station x
m, n	*See* equations (108) and (109) or equation (148)
$p =$	$(a-a_0)/\sqrt{3}$ *see also* equation (A-7)
p_{ij}	Coefficients in the expansion of ω_1, *see* equation (14)
p, q	*See* equations (162) and (170)
P	*See* equations (38) or (67)
$s(x)$	Wing semi-span
$S(x)$	Planform area, or cross-sectional area in Appendix B
$t =$	$(\alpha/4)^{1/3}$
U	Free-stream velocity
W	Complex velocity potential
W_a	Attached flow contribution to complex velocity potential
x, y, z	Rectangular cartesian coordinates aligned with the wing
x', y', z'	Rectangular cartesian coordinates aligned with the free stream
Z	Complex variable in the cross-flow plane
Z_1	Complex coordinate based on wing leading edge
Z_v	Position of the right-hand vortex in the cross-flow plane
Z^*	Complex variable in transformed plane, *see* equation (150)
α	Angle of incidence to free stream
$B(w, z)$	Beta function
Γ	Circulation about right-hand vortex
$\Gamma(x, y)$	Incomplete gamma function
γ	Non-dimensional vortex strength
δ	Leading-edge angle of rhombic wing
$\varepsilon =$	$(\pi-\delta)/2\pi$
$\varepsilon_0 =$	$\frac{1}{2}(3-\sqrt{5})$
$\eta =$	$1+\omega_v$, *see* equation (55)
η, ζ	Non-dimensional vortex coordinates in Section 4
λ, μ	*See* equation (159)
ρ	Fluid density
σ, τ	Vortex coordinates relative to leading edge in transformed plane
σ_0, τ_0	*See* equation (96)
σ_1, τ_1	*See* equation (109)
ω	Complex variable in transformed plane
ω_v	Position of right-hand vortex in transformed plane
$\omega_1 =$	ω_v/d

χ	Point of inboard-flow separation in cross-flow plane. *See also* equation (140)
μ	Point of inboard-flow separation in transformed plane
ξ	*See* equation (108)
ρ_1, ρ_2, ρ_3	*See* equations (45) or (A-10)
$\theta_1, \theta_2, \theta_3$	*See* equations (45) or (A-10)

REFERENCES

No.	Author(s)	Title, etc.
1	C. E. Brown and W. H. Michael	On slender delta wings with leading-edge separation. *Journ. Aero. Sci., 21,* 690–694 and 706, 1954, NACA TN 3430 (1955)
2	J. E. Barsby	Flow past conically-cambered slender delta wings with leading-edge separatión. ARC R & M 3748 (1972)
3	J. E. Barsby	Separated flow past a slender delta wing at low incidence. *Aeron. Quart., 24,* 2, 120–128 (1973)
4	J. H. B. Smith	Improved calculations of leading-edge separation from slender delta wings. Proc. Roy. Soc. A, *306,* 67–90 (1968), RAE Technical Report 66070 ARC 27897 (1966)
5	J. H. B. Smith	The isolated vortex model of leading-edge separation revised for small incidence. RAE Technical Report 73160 ARC 35347 (1974)
6	J. H. B. Smith	Calculations of the flow over thick, conical slender wings with leading-edge separation. ARC R & M 3694 (1971)
7	H. Portnoy and S. C. Russell	The effect of small conical thickness distributions on the separated flow past slender delta wings. ARC CP 1189 (1971)
8	H. Portnoy	The slender-wing with a half body of revolution mounted beneath. *Journ. R. Ae. Soc., 72,* 803–807 (1968)
9	E. C. Maskell	Similarity laws governing the initial growth of leading-edge vortex sheets in conical flow past sharp-edged slender bodies. X Int. Congr. Appl. Mech., Stresa (1960)
10	P. J. Davies	Assessment of the accuracy of subsonic linearised theory for the design of warped slender wings. ARC CP 1324 (1974)
11	J. H. B. Smith	A theory of the separated flow from the curved leading edge of a slender wing. ARC R & M 3116 (1957)
12	W. P. Jones	Trends in unsteady aerodynamics. 6th Lanchester Memorial Lecture, 1962 *Journ. R. Ae. Soc., 67,* 137–152 (1963)
13	R. K. Nangia and G. J. Hancock	Delta wings with longitudinal camber at low speed. ARC CP 1129 (1969)
14	M. H. Snyder	Some effects of camber on swept-back wings. Society of Automotive Engineers Paper 730298 (1973)
15	I. S. Gradshteyn and I. M. Ryzhik ...	*Table of integrals, series and products.* Academic Press (1965)

16 M. D. Van Dyke ..... *Perturbation methods in fluid mechanics.* Academic Press (1964)

17 D. A. Kirby ..... An experimental investigation of the effect of planform shape on the subsonic longitudinal stability characteristics of slender wings. ARC R & M 3568 (1967)

18 G. N. Ward ..... *Linearised theory of steady high-speed flow.* Cambridge University Press (1955)

APPENDIX A

Uniqueness of Small Vortex Solution for the Rhombic Cone

We wish to examine the possibility of the existence of solutions of equation (8) for which the vortex system tends to some point on the wing other than the leading edge in the limit as the incidence vanishes.

We introduce the functions $F(\omega)$ and $G(\omega)$ defined by

$$F(\omega)=\frac{B(\frac{1}{2}+\varepsilon,1-\varepsilon)\cos\varepsilon\pi}{\pi(1-2\varepsilon)}\frac{\omega}{(1+\omega^2)^{\varepsilon}}{}_2F_1(1-\varepsilon,\tfrac{1}{2}-\varepsilon;3/2-\varepsilon,-\omega^2) \tag{A-1}$$

where ${}_2F_1$ is a hypergeometric function, and

$$G(\omega)=\left(\frac{\omega^2}{1+\omega^2}\right)^{\varepsilon}\int_0^{\omega}\left(\frac{t^2}{1+t^2}\right)^{\varepsilon}dt \quad . \tag{A-2}$$

Using equation (C-3) from Ref. 6 we find that

$$\frac{dF}{d\omega}=\frac{2\varepsilon}{\omega(1+\omega^2)}F(\omega)+\frac{2\cos\varepsilon\pi}{\pi(1+\omega^2)}J \tag{A-3}$$

where $J=\frac{1}{2}B(\frac{1}{2}+\varepsilon,\,1-\varepsilon)$.

We can therefore expand F and G about any point ω to give

$$F(\omega+\eta)=F(\omega)+\frac{2}{1+\omega^2}\left(\frac{\varepsilon}{\omega}F(\omega)+\frac{\cos\varepsilon\pi}{\pi}J\right)\eta+0(\eta^2) \quad , \tag{A-4}$$

and

$$G(\omega+\eta)=G(\omega)+\frac{2\varepsilon}{\omega(1+\omega^2)}G(\omega)\eta+\left|\frac{\omega^2}{1+\omega^2}\right|^{2\varepsilon}\bar{\eta}+0(\eta^2) \quad . \tag{A-5}$$

Using equation (1) and equations (C-1) and (C-4) of Ref. 6, equation (8) can be written as

$$\frac{ia}{(\omega_1+\bar{\omega}_1)^2}\left(\omega_1^2+\bar{\omega}_1(\omega_1+\bar{\omega}_1)\left(1-\frac{\varepsilon}{1+\omega_1^2}\right)\right)=-F(\omega_1)-\frac{2d}{s}G(\omega_1) \quad . \tag{A-6}$$

Since we are seeking a solution for which the vortex approaches some inboard point as the incidence vanishes we write $\omega_1=ip+\eta$ where $0<p\leq 1$. We deal with the case in which $p<1$ first of all, and taking $\eta=\sigma+i\tau$ we can use the expansions given by (A-4) and (A-5) to obtain the leading terms in (A-6),

$$\begin{aligned}&\frac{ia}{4\sigma^2}\left(-p^2-2p\tau+\frac{2i\varepsilon p\sigma}{1-p^2}+0(\eta^2)\right)\\&\quad=-\left(F(ip)+\frac{2d}{s}G(ip)\right)-\frac{2}{(1-p^2)}\left(\frac{\varepsilon}{ip}\left(F(ip)+\frac{2d}{s}G(ip)\right)+\frac{\cos\varepsilon\pi}{\pi}J\right)(\sigma+i\tau)\\&\qquad-\frac{2d}{s}\left(\frac{p^2}{1-p^2}\right)^{2\varepsilon}(\sigma-i\tau)+0(\eta^2) \quad .\end{aligned} \tag{A-7}$$

Now suppose that there exists a value for p such that $0<p<1$ for which $F(ip)+(2d/s)G(ip)=0$, then we find by equating the real parts of equation (A-7) that $\sigma=0(a^{1/2})$. However equating the leading imaginary terms leads to the conclusion that $\tau=0(1)$, and so, if such a p exists it will not provide the solution we are looking for. We can therefore take $F(ip)+(2d/s)G(ip)$ to be non-zero, and we note that it will in fact be purely imaginary. Again we can equate the leading imaginary terms to find that

$$\frac{iap^2}{4\sigma^2}=F(ip)+\frac{2d}{s}G(ip) \quad , \tag{A-8}$$

and substituting this back into equation (A-7) and equating the leading real terms gives

$$\frac{\cos \varepsilon\pi}{\pi(1-p^2)}J+\frac{d}{s}\left(\frac{p^2}{1-p^2}\right)^{2\varepsilon}=0 \quad . \tag{A-9}$$

Now since $0<p<1$ both terms in this equation will be positive and there can be no solution for p in the required range. We can therefore conclude that there can be no solution for which the vortex approaches a point on the wing surface away from the centre line and the leading edge.

It only remains to examine the possibility that the vortex might tend to the wing centre line as the incidence vanishes. This will involve expanding the expressions for F and G given by (A-1) and (A-2) about the point $\omega_1 = i$ and since $(1+\omega_1^2)^{\varepsilon}$ will be many-valued at this point it will be necessary to specify which root should be chosen to ensure that F and G are single-valued. If we write

$$\omega_1 - i = \rho_1 \mathrm{e}^{i\theta_1} \quad ,$$
$$\omega_1 + i = \rho_2 \mathrm{e}^{i\theta_2}$$

and

$$\omega_1 = \rho_3 \mathrm{e}^{i\theta_3} \tag{A-10}$$

and constrain ω_1 to lie on the sheet of the Riemann surface for which θ_1, θ_2 and θ_3 all lie in the range $[-(\pi/2), \pi/2]$ then using

$$\frac{dZ}{d\omega} = \left(\frac{\omega_1^2}{\omega_1^2+1}\right)^{\varepsilon}$$
$$= \left(\frac{\rho_3^2}{\rho_1\rho_2}\right)^{\varepsilon} \mathrm{e}^{i(2\theta_3-\theta_1-\theta_2)\varepsilon} \tag{A-11}$$

we can verify that the transformation will correctly map the boundary of the right-hand half of the ω-plane, *DABCD* in Fig. 2b into the imaginary axis and wing cross-section *DABCD* in Fig. 2a.

We can now make use of the properties of the hypergeometric and beta functions to expand equations (A-1) and (A-2) for small ρ_1 to obtain

$$F(i+\rho_1 \mathrm{e}^{i\theta_1}) \sim \frac{1}{(2\rho_1)^{\varepsilon}} \operatorname{cosec} \pi\varepsilon \, \mathrm{e}^{i((\pi/2)(1-\varepsilon)-\varepsilon\theta_1)} \tag{A-12}$$

and

$$\frac{2d}{s}G(i+\rho_1 \mathrm{e}^{i\theta_1}) \sim -\frac{2}{(2\rho_1)^{\varepsilon}} \operatorname{cosec} \pi\varepsilon \, \mathrm{e}^{i((\pi/2)(1-\varepsilon)-\varepsilon\theta_1)} \quad , \tag{A-13}$$

where we have also applied equation (1).

If we write $\omega_1 = i+\sigma+i\tau$ where σ and τ are both real and small then we can expand the left-hand side of equation (A-6) and apply equations (A-12) and (A-13) to give

$$\frac{a\varepsilon\tau}{4\sigma(\sigma^2+\tau^2)} - \frac{ia((1-\varepsilon)\sigma^2+\tau^2)}{4\sigma^2(\sigma^2+\tau^2)} \sim \frac{\operatorname{cosec} \varepsilon\pi}{(2\rho_1)^{\varepsilon}} \mathrm{e}^{i((\pi/2)(1-\varepsilon)-\varepsilon\theta_1)} \quad . \tag{A-14}$$

Now since $|\theta_1| \leq \pi/2$ and $0<\varepsilon<\frac{1}{2}$ it follows that $0<\pi/2(1-\varepsilon)-\varepsilon\theta_1 \leq \pi/2$ and so the imaginary part of the right-hand side of equation (A-14) must be positive. However the imaginary part of the left-hand side is clearly negative and there can be no solution satisfying this equation, and hence no solution in which the vortex approaches the centre line as the incidence vanishes.

The only valid small incidence approximation must therefore be that given by equation (13) for which the vortex tends to the leading edge as the incidence vanishes.

APPENDIX B

Calculation of the Lift on the Half-Circular Cone

The lateral force on a slender body is given by Ward[18] in terms of the axes $0x'y'z'$ aligned with the free stream. If we assume that the incidence is small then the coordinates with respect to these new axes will be related to those of Section 3 by

$$x' = x + \alpha z \quad ,$$
$$y' = y$$

and

$$z' = -\alpha x + z \quad . \tag{B-1}$$

We write $Z' = y' + iz'$, and let $Z'_g(x')$ be the value of Z' at the centre of area of the wing cross-section at the station x'. The lateral force in this cross-sectional plane is now given by equation (9.7.11) of Ref. 18 as

$$\frac{F}{\frac{1}{2}\rho U^2} = 4\pi c + 2\frac{d}{dx'}(Z'_g(x')S(x')) \tag{B-2}$$

where $S(x')$ is the cross-sectional area in the plane $x' =$ constant and c is the coefficient of $1/Z'$ in the expansion of $W/U + i\alpha Z$ for large $|Z'|$.

The conformal transformation given by equation (44) maps the point at infinity in the Z-plane to the point $\omega = i/\sqrt{3}$, and so if we write

$$\omega = i(1+\eta)/\sqrt{3} \tag{B-3}$$

$|Z|$ large will correspond to small $|\eta|$. Also, for small $|\eta|$, we can find expansions for $1/\eta$ and W in the form

$$\frac{1}{\eta} = b_0\frac{Z}{s}\left(1 + b_1\frac{s}{Z} + b_2\frac{s^2}{Z^2} + 0\left(\frac{s^3}{Z^3}\right)\right) \quad , \tag{B-4a}$$

$$\frac{W}{U} = \frac{a_0}{\eta} + a_1 \ln \eta + a_2 + a_3\eta + 0(\eta^2) \quad . \tag{B-4b}$$

Combining these two expressions leads to

$$W/U + i\alpha Z = \left(\frac{a_0 b_0}{s} + i\alpha\right)Z - a_1 \ln Z + a_2 + a_0 b_0 b_1 + \left(a_0 b_0 b_2 - a_1 b_1 + \frac{a_3}{b_0}\right)\frac{s}{Z} + 0\left(\frac{1}{Z^2}\right) \quad , \tag{B-5}$$

and making the further approximation $Z = Z'(1 + i\alpha x/Z')$ which follows from equations (B-1) we can show that

$$c = a_0 b_0 b_2 s + a_3 s/b_0 - a_1 b_1 s - i\alpha a_1 x \quad . \tag{B-6}$$

From the transformation (44) we can expand ω in terms of $1/Z$ for large Z to give

$$\omega = \frac{i}{\sqrt{3}}\left(1 + \frac{8i}{3\sqrt{3}}\frac{s}{Z} - \frac{16}{27}\frac{s^2}{Z^2} + \frac{8i}{81\sqrt{3}}\frac{s^3}{Z^3} + \ldots\right) \quad , \tag{B-7}$$

so that with the aid of equation (B-3) we can derive an expansion for $1/\eta$ from which we find that the constants involved in equation (B-4a) are

$$b_0 = -\frac{3\sqrt{3}}{8}i \quad , \qquad b_1 = -\frac{2\sqrt{3}}{9}i \quad , \qquad b_2 = -\frac{5}{27} \quad . \tag{B-8}$$

The expression (48) for the complex conjugate velocity can also be expanded for small η using equation (B-3) to obtain

$$\frac{1}{KUs}\frac{dW}{d\omega} = \frac{8ai}{3\eta^2} + \frac{\sqrt{3}i}{2\eta} - \left(\frac{2a}{3} + \frac{\sqrt{3}}{2}\right)i - \frac{\gamma}{\sqrt{3}\pi}\left(\frac{1}{\omega_v^2 + 1/3} - \frac{1}{\bar{\omega}_v^2 + 1/3}\right) + 0(\eta) \tag{B-9}$$

which can be integrated to determine the remaining constants involved in equation (B-6). Thus

$$a_0 = \frac{8aKs}{3\sqrt{3}} \quad , \qquad a_1 = -\tfrac{1}{2}Ks \quad , \qquad a_3 = \left(\frac{2a}{3\sqrt{3}} + \frac{1}{2}\right)Ks + \frac{K\gamma s}{3\pi i}\left(\frac{1}{\omega_v^2 + 1/3} - \frac{1}{\bar{\omega}_v^2 + 1/3}\right) \quad . \tag{B-10}$$

Now the centre of area for the wing cross section is at a distance $4s/3\pi$ below the upper surface so that

$$Z_g' = -\left(\frac{4K}{3\pi} + \alpha\right)ix \quad . \tag{B-11}$$

Also to the order of approximation used here

$$S(x') = S(x) = \tfrac{1}{2}\pi K^2 x^2 \tag{B-12}$$

and we can write

$$\frac{d}{dx'}(Z_g' S(x')) = -2Ks^2 i - \frac{3}{2}\pi aKs^2 i \quad . \tag{B-13}$$

Therefore, combining equations (B-6), (B-8), (B-10) and (B-13) in equation (B-2) the lateral force is given by

$$\frac{F}{\frac{1}{2}\rho U^2} = \frac{19Ks^2\pi}{3\sqrt{3}}ip + \frac{13Ks^2\pi}{8\sqrt{3}}i - 4Ks^2 i + \frac{32K\gamma s^2}{9\sqrt{3}}\left(\frac{1}{\omega_v^2 + 1/3} - \frac{1}{\bar{\omega}_v^2 + 1/3}\right) \quad . \tag{B-14}$$

Using the planform area s^2/K to define the lift coefficient C_L, and using equations (49) and (54) to replace γ gives

$$\frac{C_L}{K^2} = \frac{13\pi}{8\sqrt{3}} - 4 + \frac{19\pi}{3\sqrt{3}}p + \frac{64\pi(1-\omega_v^2)(1-\bar{\omega}_v^2)}{9\sqrt{3}(\omega_v^2 + 1/3)(\bar{\omega}_v^2 + 1/3)}p \quad . \tag{B-15}$$

At the attachment incidence $p = 0$ and so the first two terms will give the lift at this incidence. The first three terms agree with the expression given by Portnoy[8]. The last term is the non-linear lift due to the vortex system, and can be further simplified using the asymptotic behaviour for ω_v given by equations (55) and (59), so that we find

$$\frac{C_L}{K^2} = \frac{13\pi}{8\sqrt{3}} - 4 + \frac{19\pi}{3\sqrt{3}}p + \frac{640\pi}{27\sqrt{3}}p^3 \quad . \tag{B-16}$$

TABLE 1

Vortex Position in the Transformed Plane: $Z_v^* = s(Ax^p + iBx^q)$

Planform	Camber	p	q	A	B
Delta: $A_0 = 0,\ A_1 > 0$	$n > 0$	$\frac{2n}{3}$	$\frac{n}{3}$	$\left(\frac{K_1 B}{4A_1}\right)^{1/2}$	$\left(\frac{K_1}{4(n+1)A_1}\right)^{1/3}$
Rectangular: $A_0 > 0,\ A_1 = 0$ (streamwise tip)	$n > 0$	$\frac{n+1}{3}$	$\frac{n+1}{3}$	$\left(\frac{K_1}{4(2n+1)A_0}\right)^{1/3}$	$\left(\frac{K_1}{4(2n+1)A_0}\right)^{1/3}$
Tip raked-in or out: $A_0 > 0,\ A_1 \neq 0$	$0 < n < \frac{1}{2}$	$\frac{n+1}{3}$	$\frac{n+1}{3}$	$\left(\frac{K_1}{4(2n+1)A_0}\right)^{1/3}$	$\left(\frac{K_1}{4(2n+1)A_0}\right)^{1/3}$
Tip raked-in or out: $A_0 > 0,\ A_1 \neq 0$	$n = \frac{1}{2}$	$\frac{1}{2}$	$\frac{1}{2}$	$B_0\left(\frac{K_1}{K_1 + 4A_1 B_0}\right)^{1/2}$	B_0
Tip raked out: $A_0 > 0,\ A_1 > 0$	$n > \frac{1}{2}$	$\frac{4n+1}{6}$	$\frac{n+1}{3}$	$\left(\frac{K_1 B}{4A_1}\right)^{1/2}$	$\left(\frac{K_1}{2(2n+1)A_0}\right)^{1/3}$
Tip raked in: $A_0 > 0,\ A_1 < 0$	$n > \frac{1}{2}$	$\frac{1}{2}$	n	$\left(\frac{4A_1}{(2n+3)A_0}\right)^{1/2}$	$\frac{(2n+3)K_1}{8(2n+1)A_1}$

(for B_0, see equation (192))

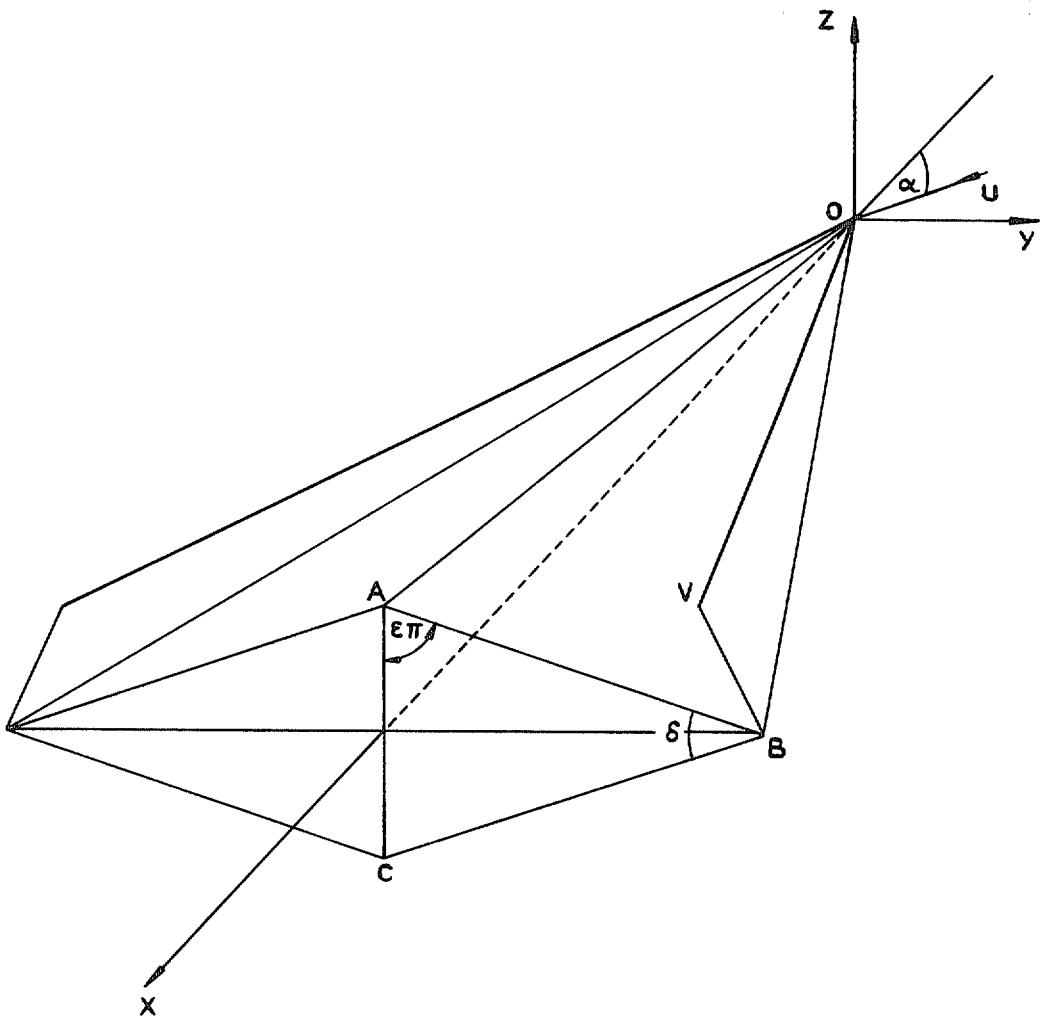

FIG. 1. Wing and coordinate system.

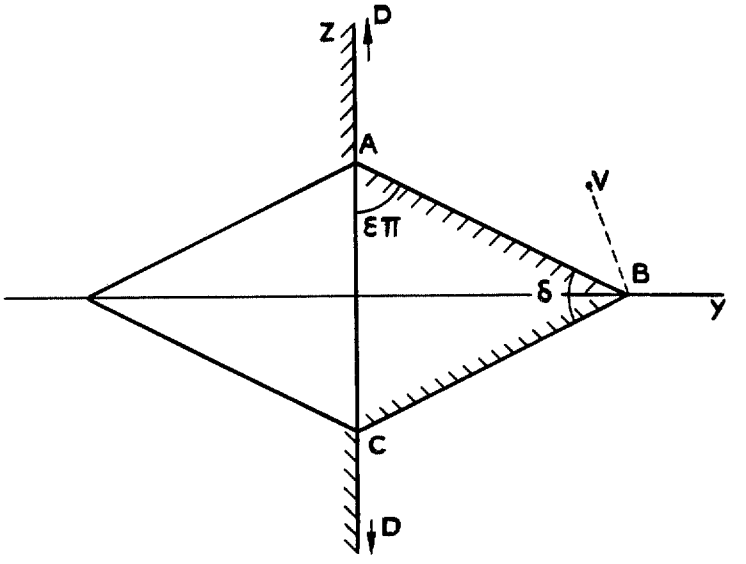

FIG. 2a. Wing cross-section in Z-plane.

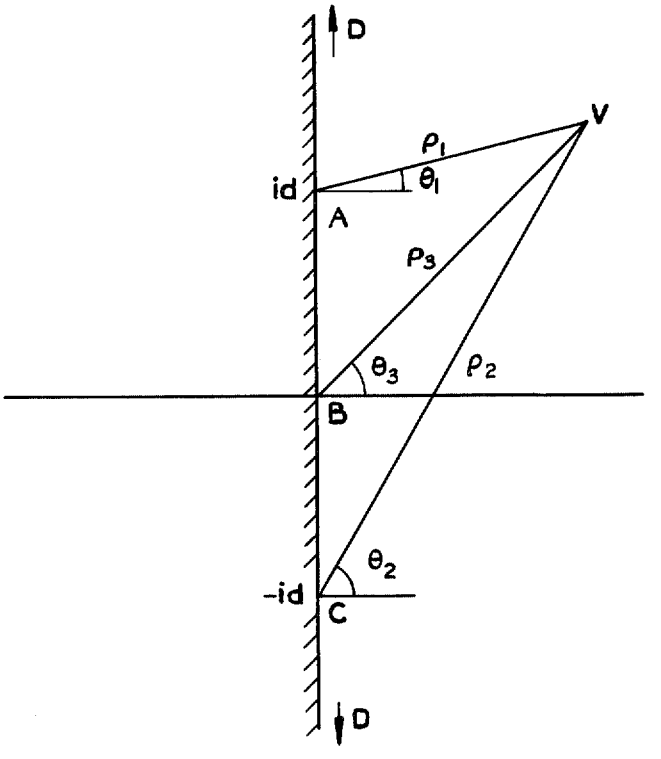

FIG. 2b. Wing cross-section in ω-plane.

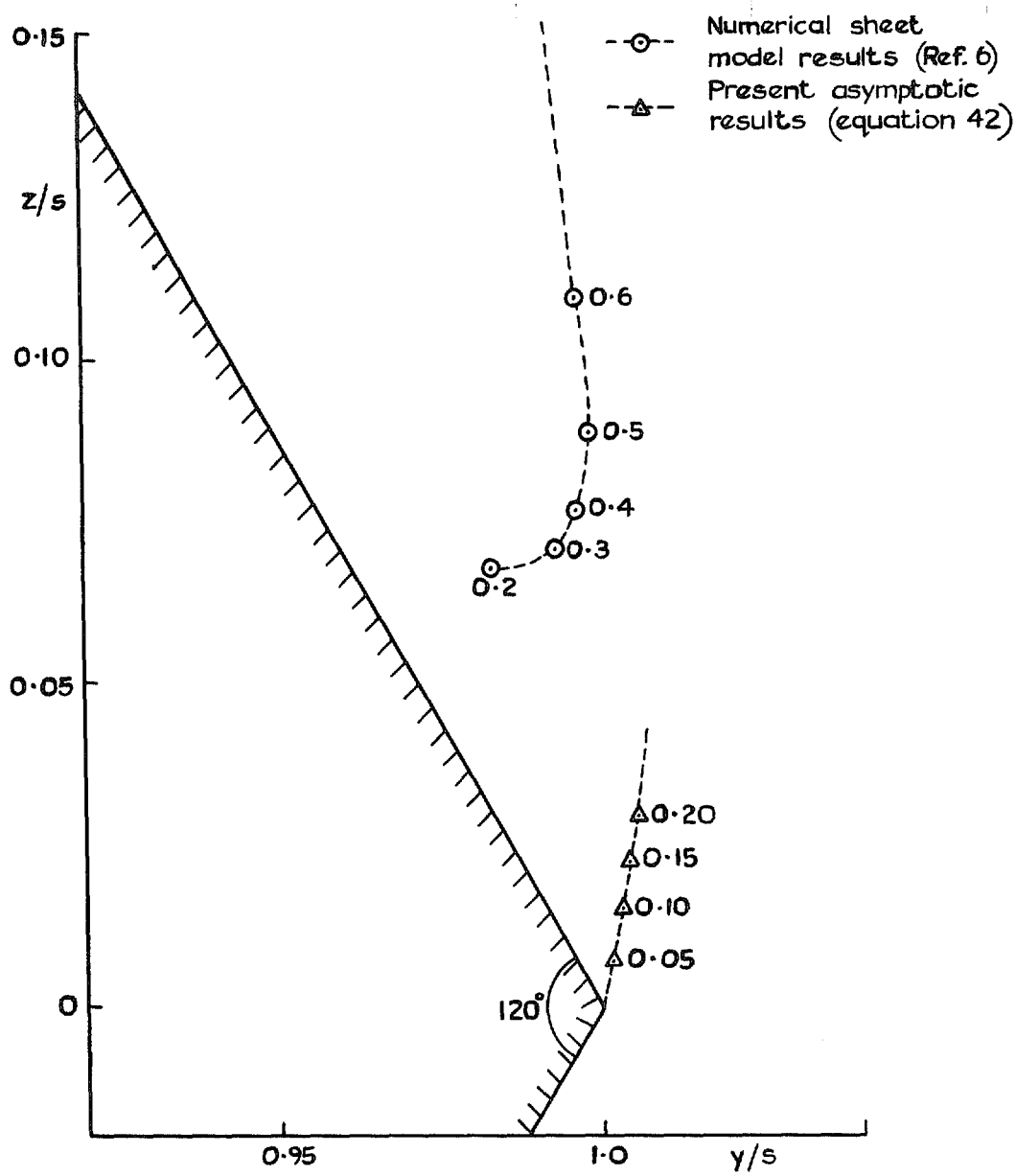

FIG. 3. Variation of isolated vortex position with a.

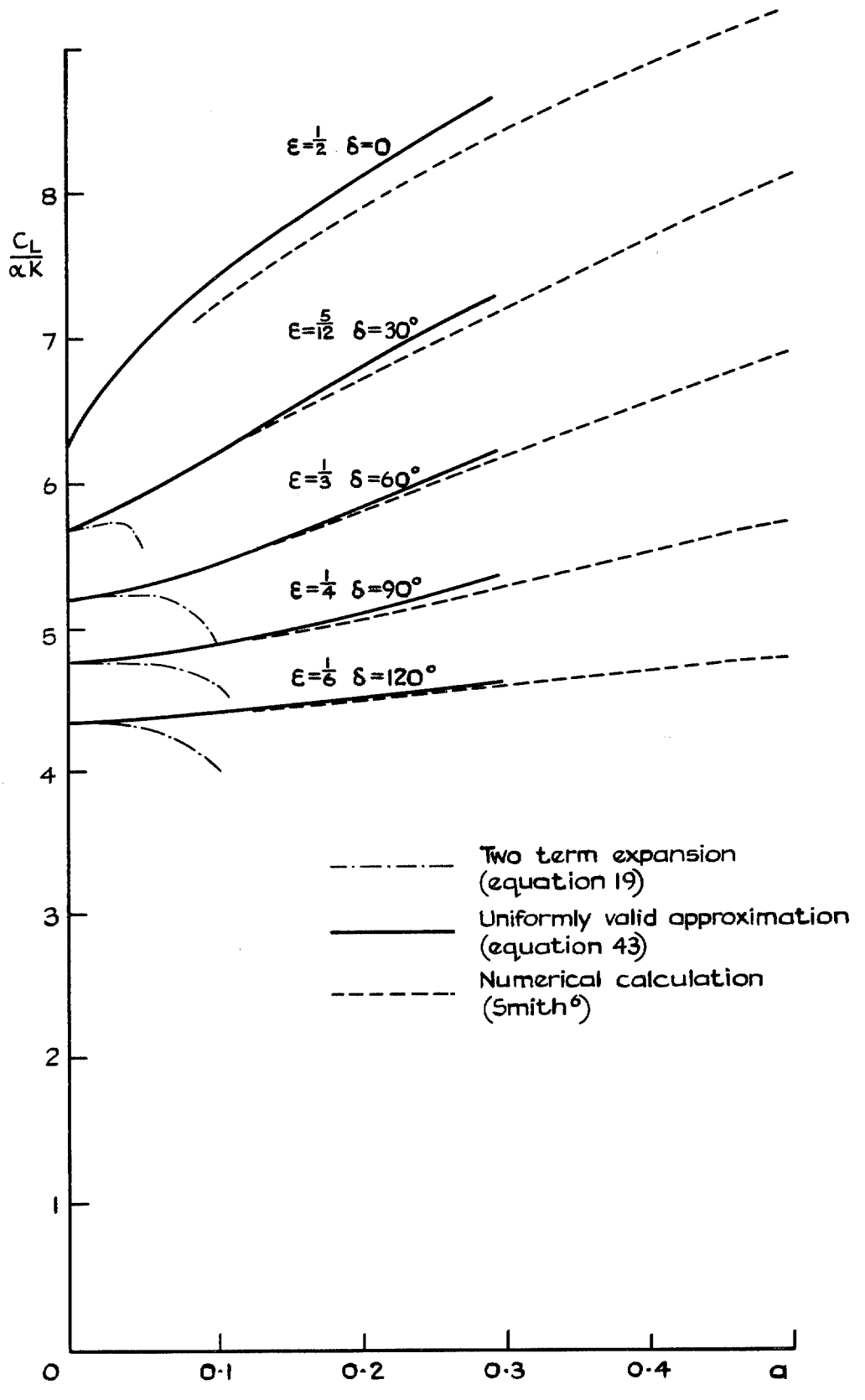

FIG. 4. Lift coefficient on rhombic wing.

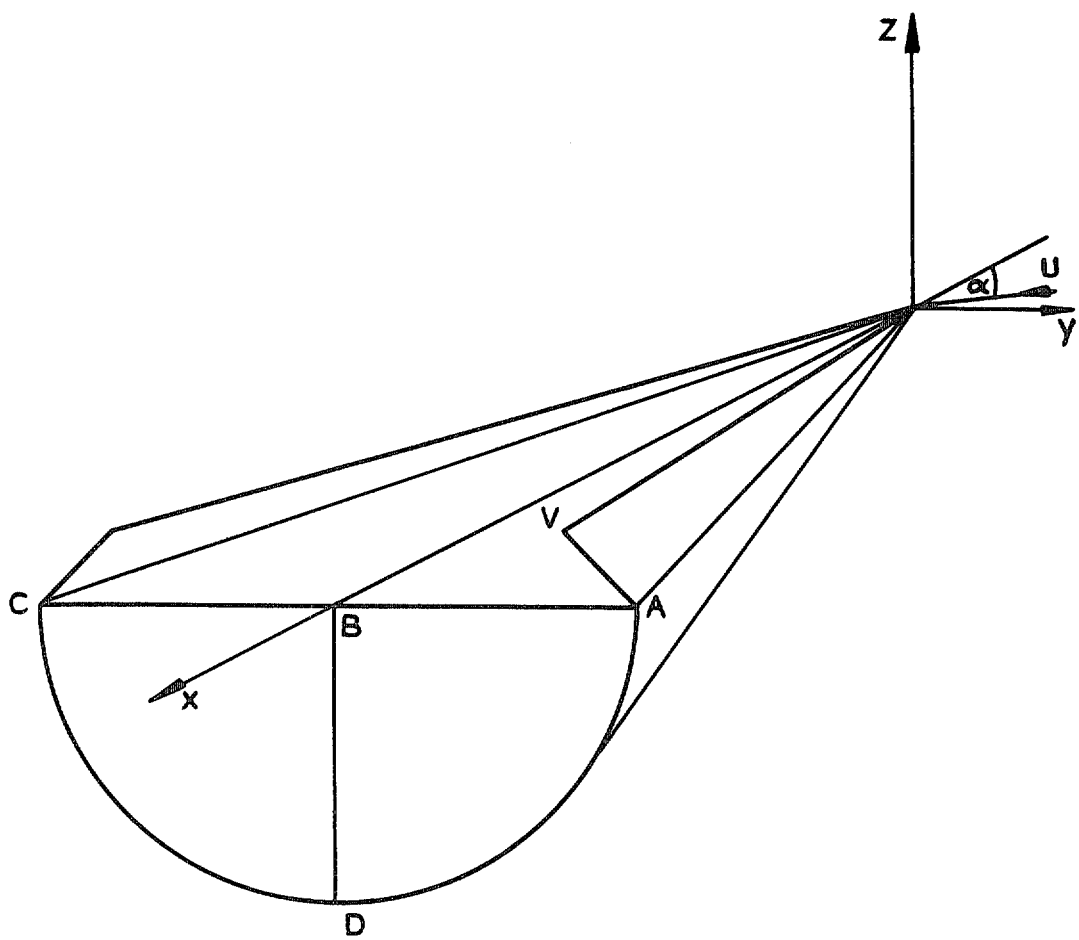

FIG. 5. Wing and coordinate system.

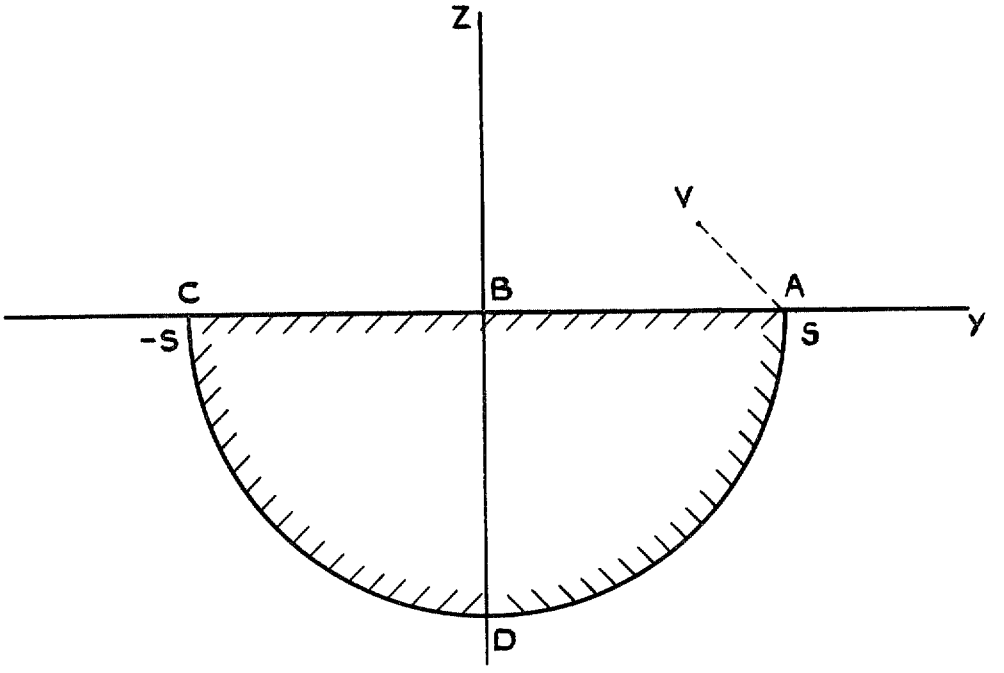

FIG. 6a. Wing cross-section in Z-plane.

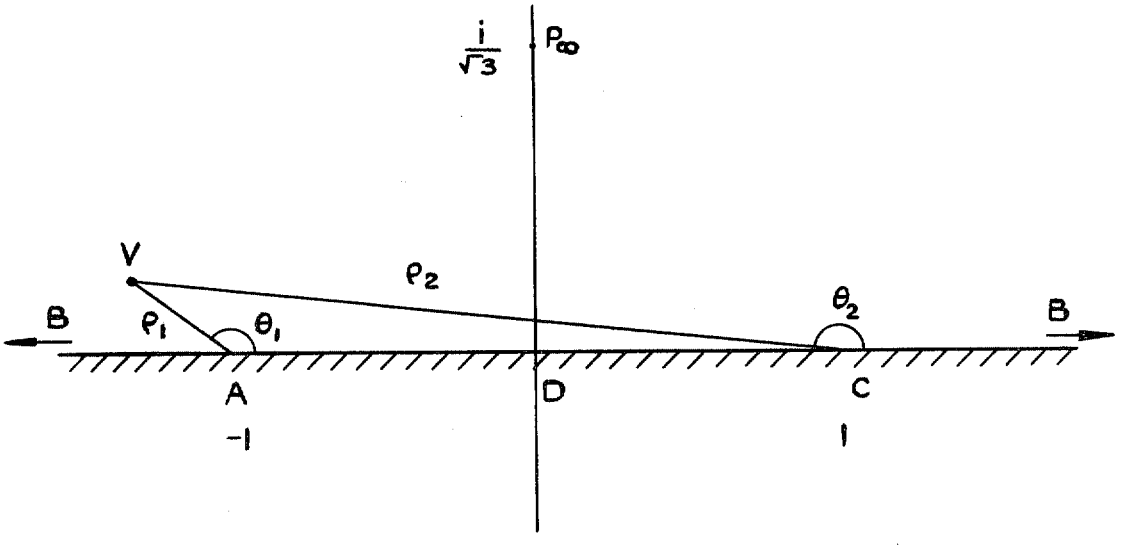

FIG. 6b. Wing cross-section in ω-plane.

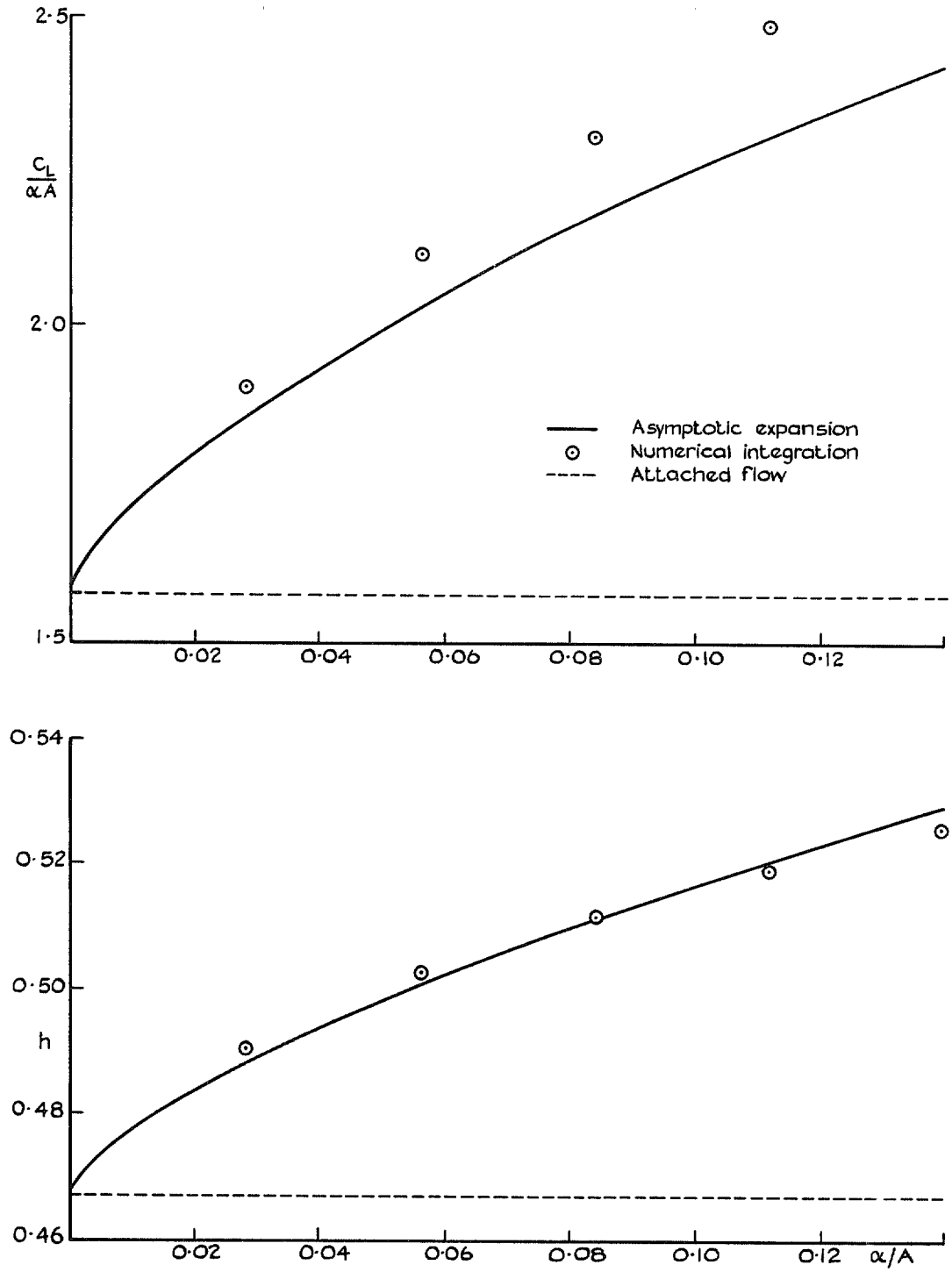

FIG. 7. Lift and centre of pressure of flat-plate gothic wings.

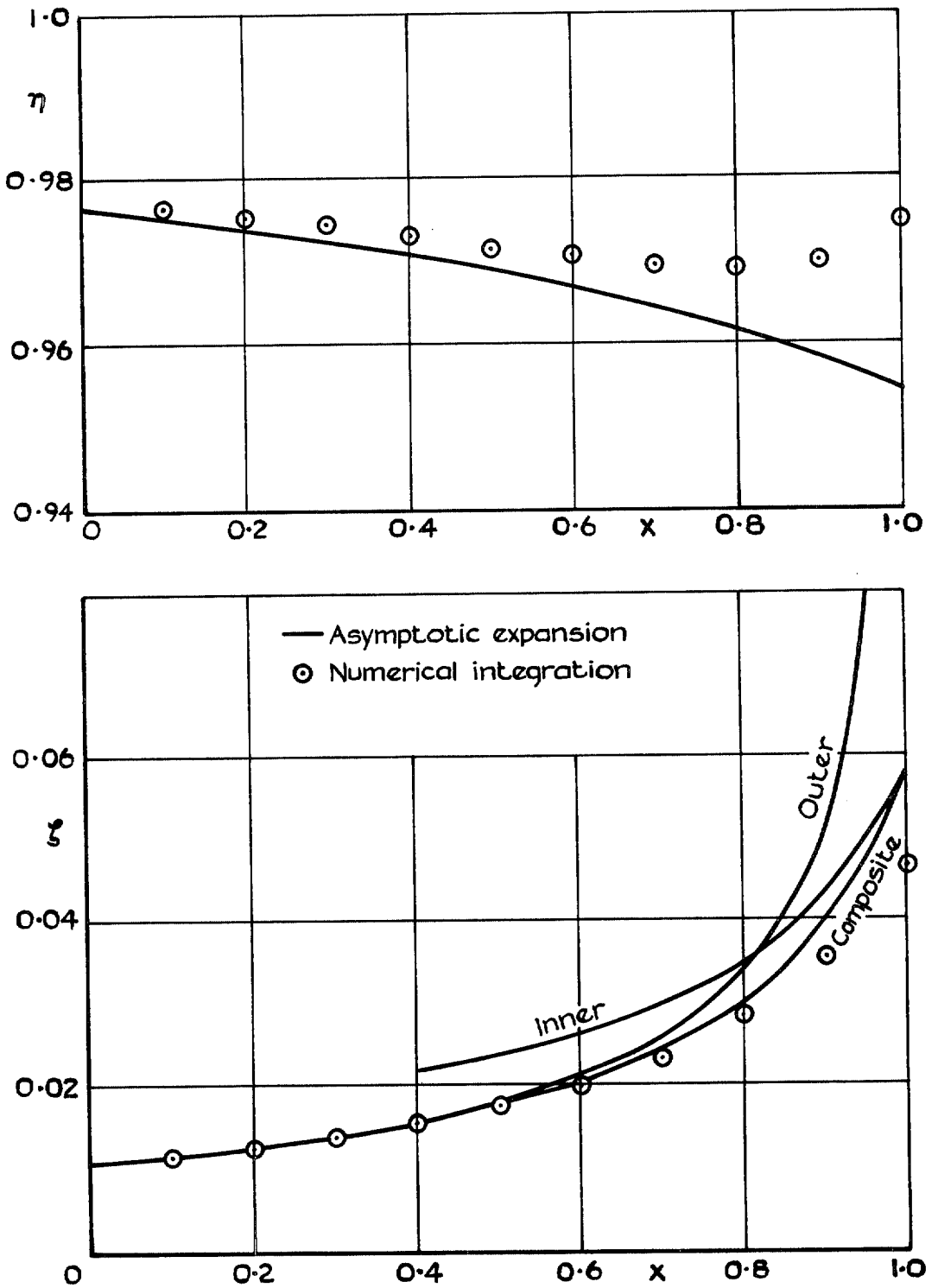

FIG. 8. Vortex position on flat-plate gothic wing at $\frac{\alpha}{A} = 0{\cdot}0279$. (e.g. $\alpha = 2°$, $A = 1{\cdot}25$)

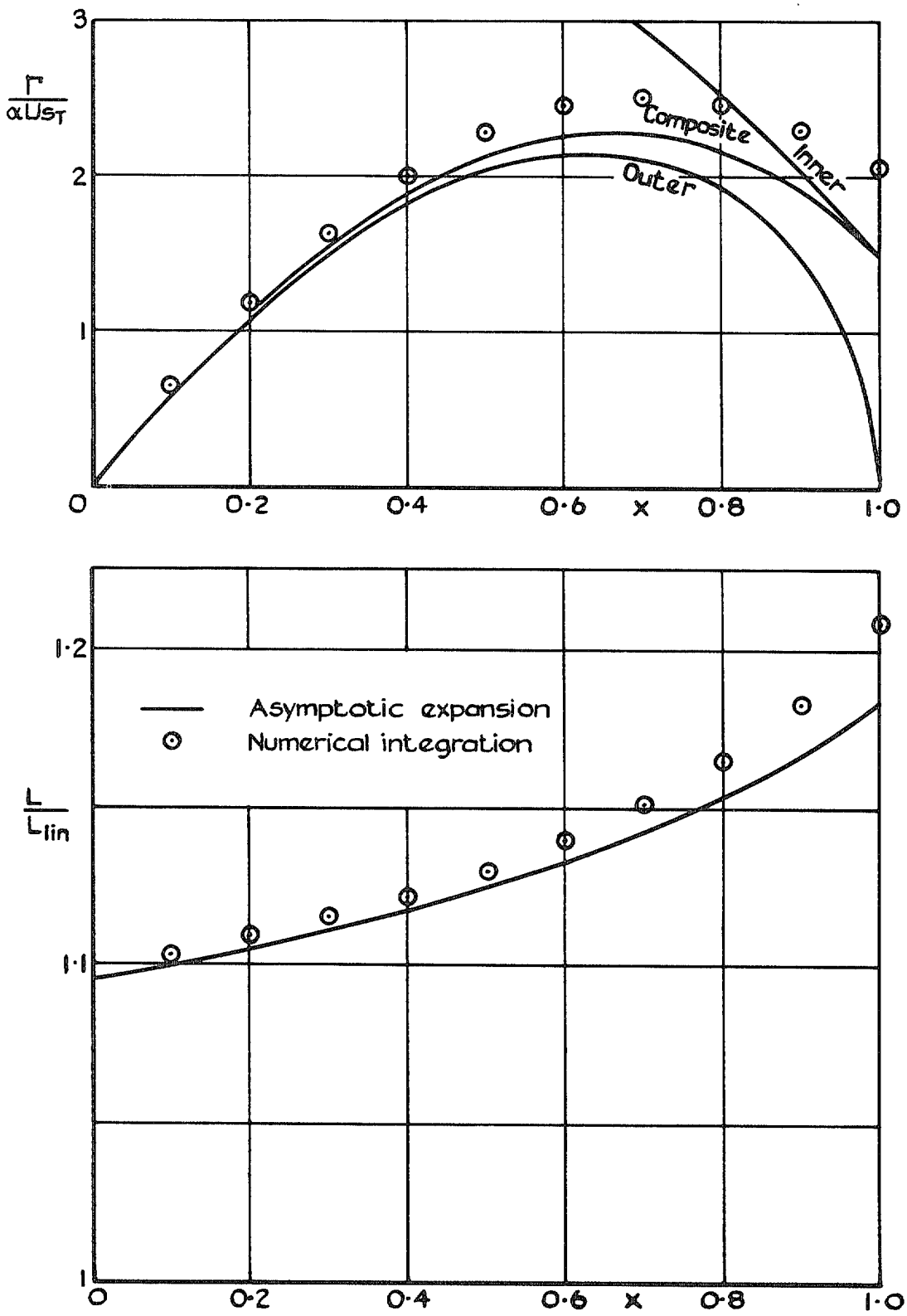

FIG. 9. Vortex strength and nonlinear lift distribution for flat-plate gothic wing at $\alpha/A = 0{\cdot}0279$.

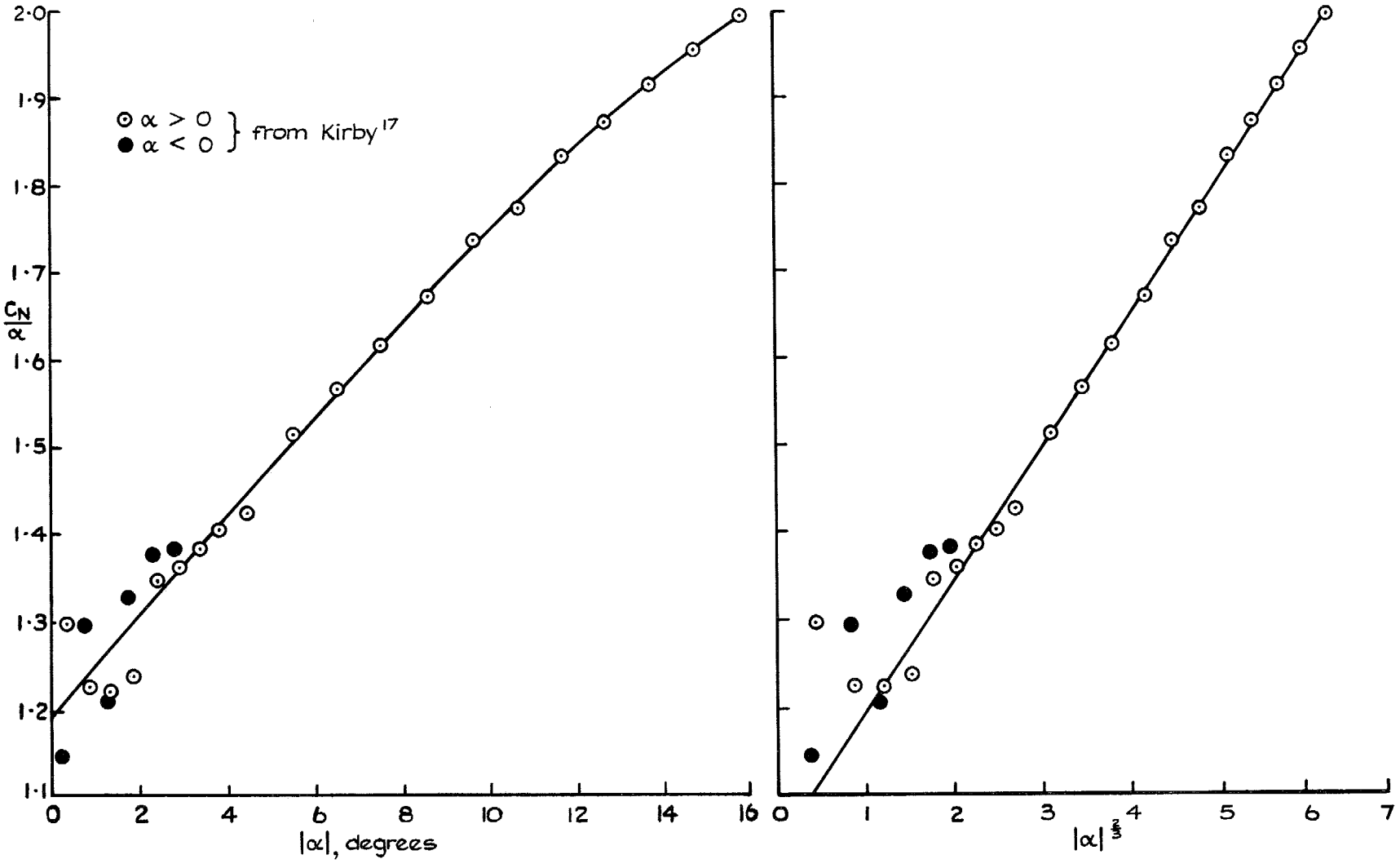

FIG. 10. Alternative extrapolations of C_N/α for delta wing of aspect ratio one.

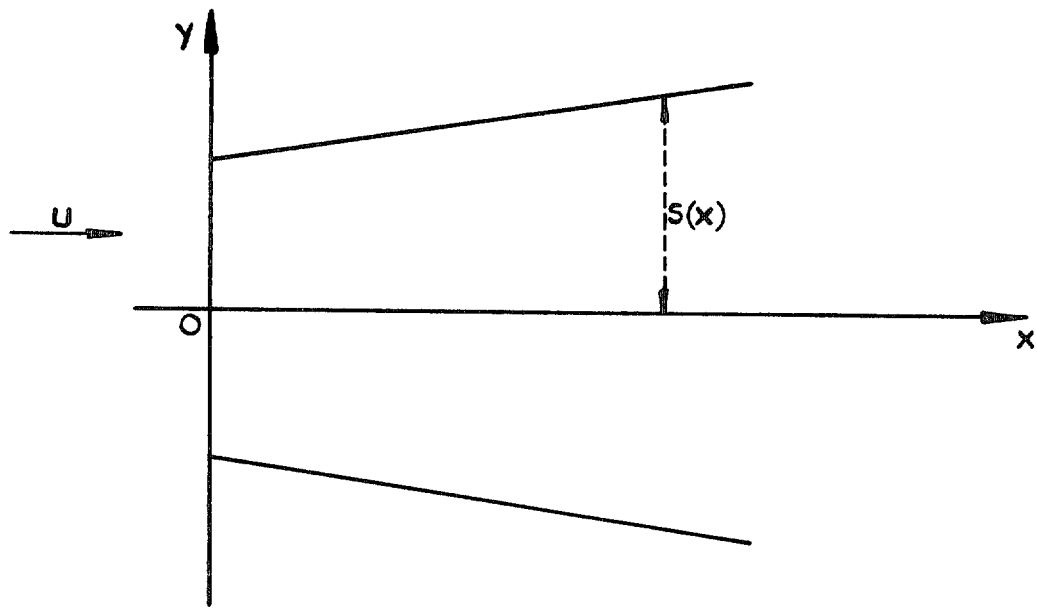

FIG. 11a. Planform of truncated delta wing.

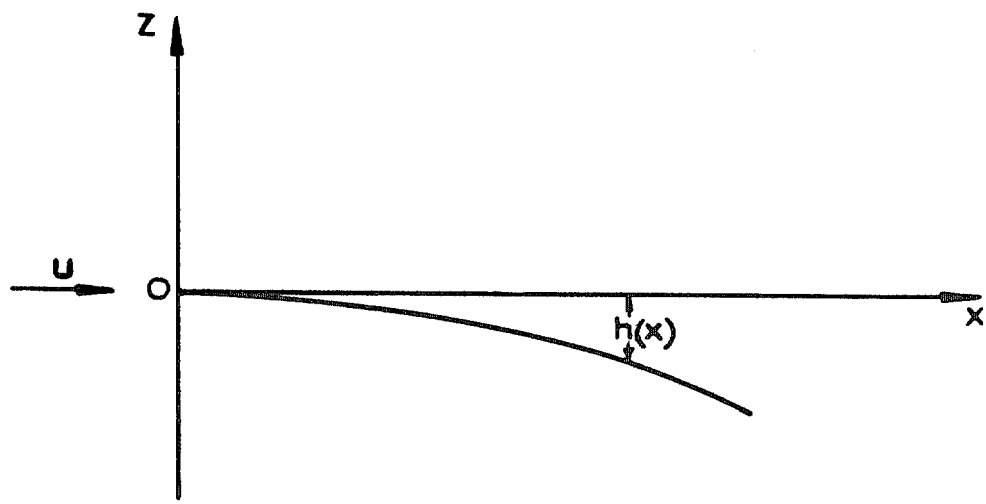

FIG. 11b. Side view of truncated delta wing.

Printed in England for Her Majesty's Stationery Office by J. W. Arrowsmith Ltd., Bristol BS3 2NT
Dd. 289031 K5 8/76

© *Crown copyright* 1976

HER MAJESTY'S STATIONERY OFFICE

Government Bookshops

49 High Holborn, London WC1V 6HB
13a Castle Street, Edinburgh EH2 3AR
41 The Hayes, Cardiff CF1 1JW
Brazennose Street, Manchester M60 8AS
Southey House, Wine Street, Bristol BS1 2BQ
258 Broad Street, Birmingham B1 2HE
80 Chichester Street, Belfast BT1 4JY

Government Publications are also available through booksellers

ISBN 0 11 470956 4